Immunology
The Journal of cells, molecules, systems and technologies
British Society for immunology

IMMUNOLOGY ORIGINAL ARTICLE

Induction of hepatitis B virus surface antigen-specific cytotoxic T lymphocytes can be up-regulated by the inhibition of indoleamine 2, 3-dioxygenase activity

Hiroyasu Ito,[1] Tatsuya Ando,[1] Kazuki Ando,[1] Tetsuya Ishikawa,[3] Kuniaki Saito,[4] Hisataka Moriwaki[2] and Mitsuru Seishima[1]

[1]*Department of Informative Clinical Medicine, Gifu University Graduate School of Medicine, Gifu,* [2]*First Department of Internal Medicine, Gifu University Graduate School of Medicine, Gifu,* [3]*Department of Medical Technology, Nagoya University School of Health Sciences, Nagoya, Aichi, and* [4]*Human Health Sciences, Graduate School of Medicine and Faculty of Medicine, Kyoto University, Kyoto, Japan*

doi:10.1111/imm.12274
Received 18 December 2013; revised 19 February 2014; accepted 24 February 2014.
Correspondence: Dr Hiroyasu Ito, Department of Informative Clinical Medicine, Gifu University Graduate School of Medicine, 1-1 Yanagido, Gifu 501-1194, Japan.
Email: hito@gifu-u.ac.jp
Senior author: Mitsuru Seishima, email: seishima@gifu-u.ac.jp

Summary

Cytotoxic T lymphocytes (CTLs) are thought to be major effectors involved in viral clearance during acute infections, including hepatitis B virus (HBV) infection. A persistent HBV infection is characterized by a lack of or a weak CTL response to HBV, which may be reflective of tolerance to HBV. Efficient induction of HBV-specific CTLs leads to the clearance of HBV in patients with a chronic HBV infection. Previously, we reported that α-galactosylceramide (α-GalCer), a specific natural killer T (NKT) cell agonist, enhanced the induction of HBV surface antigen (HBsAg)-specific CTLs. In the present study, we found that inhibition of indoleamine 2,3-dioxygenase (IDO) activity enhanced the induction of HBsAg-specific CTLs after immunization with HBsAg and α-GalCer. The administration of HBsAg and α-GalCer increased the production of interleukin-2 and interleukin-12b, which are crucial for the induction of HBsAg-specific CTLs. The production of these cytokines was more strongly enhanced in IDO knockout mice compared with wild-type mice. In addition, α-GalCer induced the production of IDO in $CD11b^+$ cells, and these cells inhibited proliferation of HBsAg-specific CTLs. Our results lead to strategies for improving the induction of HBsAg-specific CTLs.

Keywords: 3-dioxygenase; cytotoxic T lymphocyte; hepatitis B virus. indoleamine 2; vaccination.

Introduction

Cytotoxic T lymphocytes (CTLs) have been shown to play a critical role in viral clearance in many types of viral infection.[1,2] Antigen-specific CTLs are generated during the T cytotoxic type 1 (Tc1) immune response, which is important in the immune response to hepatitis B virus (HBV). However, clearance of, or at least a continuous suppression of, HBV is not observed in all cases of chronic hepatitis, possibly, because of a weak CTL response to the HBV surface antigen (HBsAg). Therefore, devising an effective therapy for chronic hepatitis B requires elucidation of the mechanism underlying the weakness of the CTL response to HBsAg. Previous reports demonstrated that α-galactosylceramide (α-GalCer), a ligand for $V\alpha14^+$ natural killer T (NKT) cells, strongly induced the generation of antigen-specific CTLs.[3,4] Immunization with HBsAg plus α-GalCer enhanced the induction and proliferation of HBsAg-specific CTLs.[5] Moreover, immunization with HBsAg plus α-GalCer enabled the induction of HBsAg-specific CTLs even in HBsAg transgenic (HBsAg-Tg) mice, which generate an extremely tolerant cellular and humoral immune response to HBsAg. Hence, we decided to examine the HBsAg-specific CTL response generated in HBsAg-Tg mice following immunization with α-GalCer and HBsAg. This experiment required direct stimulation by HBsAg *in vitro*, because a sufficient number of HBsAg-specific CTLs may be difficult to induce in HBsAg-Tg mice *in vivo*.

Indoleamine 2, 3-dioxygenase (IDO) is an enzyme that participates in the catabolism of the essential amino acid L-tryptophan to L-kynurenine and is a potent immunomodulator.[6,7] This enzyme is expressed in epithelial cells, macrophages and dendritic cells and is induced by proinflammatory cytokines, including type I and type II interferons (IFN).[8–10] The binding of cytotoxic T lymphocyte antigen-4 to CD80/CD86 on the surface of dendritic cells also stimulates transcription and activity of IDO.[11,12] Our previous study demonstrated that IDO expression was enhanced by treatment of mice with α-GalCer.[13]

Although the co-administration of HBsAg and α-GalCer enhanced the induction of HBsAg-specific CTLs, the α-GalCer-induced IDO may inhibit the induction of the CTLs to some extent. Hence, in the absence of IDO, immunization with the HBsAg-α-GalCer combination may elicit a strong antigen-specific Tc1 response and numerous HBsAg-specific CTLs.

In this work, we examined the effect of IDO on the induction and proliferation of HBsAg-specific CTLs in mice immunized with α-GalCer and HBsAg. Our results indicate that elimination of IDO activity enhances the antigen-specific Tc1 response and increases the number of HBsAg-specific CTLs in mice immunized with HBsAg plus α-GalCer.

Materials and methods

Mice

Wild-type (WT) male B10.D2 (H-2^d) mice (age 8–10 weeks; weight 25–30 g) were obtained from Japan SLC Inc. (Shizuoka, Japan). IDO knockout (KO) mice on a C57BL/6J background were obtained from Jackson Laboratory (Bar Harbor, ME) and backcrossed with B10.D2 (H-2^d) mice. All procedures were conducted in accordance with the National Institutes of Health Guide for the Care and Use of Laboratory Animals, and with the guidelines for the care and use of animals established by the Animal Care and Use Committee of Gifu University, Japan.

Cell lines and reagents

The H-2^d mastocytoma cell line P815 was obtained from the American Type Culture Collection (Rockville, MD). P815 cells expressing HBV-preS1, 2 and S regions (P815preS1) and the HBsAg-specific $CD8^+$ CTL clone 6C2 were generously provided by Francis V. Chisari.[14,15] The HBsAg peptide S_{28-39} was synthesized at KURABO (Osaka, Japan). α-GalCer was obtained from Funakoshi Co. Ltd. (Tokyo, Japan) and stored as a 200 μg/ml stock solution in vehicle (0.5% weight/volume polysorbate-20). 1-methyl-D-L-tryptophan (1-MT) was purchased from Sigma-Aldrich (St Louis, MO).

ELISPOT assay

The WT and IDO-KO mice were intraperitoneally inoculated with either HBsAg (10 μg/mouse) or HBsAg (10 μg/mouse) plus α-GalCer (2 μg/mouse). Single-cell suspensions were prepared from the whole spleen on day 7 after the inoculation. A total of 2.0×10^5 splenocytes/well were stimulated for 14–16 hr with 0, 0.1 or 1 μg/ml of HBsAg peptide (S_{28-39}) in 96-well MultiScreen filter plates (Millipore, Billerica, MA) pre-coated with a rat anti-IFN-γ monoclonal antibody (mAb; R4-6A2; BD Biosciences, Franklin Lakes, NJ). The plates were washed and then incubated with a biotinylated polyclonal goat anti-IFN-γ antibody (R&D Systems, Minneapolis, MN) and, after that, with streptavidin–alkaline phosphatase. Spots were visualized by the addition of a 5-bromo-4-chloro-3-indolyl phosphatase solution (Sigma-Aldrich) and counted manually under a microscope (× 40 magnification). The number of cytokine-secreting cells was determined by a single blinded observer, and all data were generated by analysing three separate wells per sample.

Detection of HBsAg-specific CTLs by flow cytometry

Immunodominant HBsAg-specific CTLs in mice are known to be restricted by H-$2L^d$ of MHC class I, and the shortest peptide that can show the maximal activity is HBsAg S_{28-39}, sequence IPQSLDSWWTSL.[14] The number of HBsAg-specific CTLs was assessed by flow cytometry, as described previously.[16] Peptide-loaded recombinant soluble dimeric murine H-$2L^d$:Ig (mouse IgG1; BD PharMingen, San Diego, CA) was prepared by mixing soluble dimeric H-$2L^d$:Ig for 48 hr at 4° with a 160-fold molar excess of HBsAg S_{28-39}. The peptide-loaded dimeric immunoglobulins were then incubated with $CD8^+$ T cells isolated from either immunized or re-stimulated splenocytes.[16] After incubation for 1 hr at 4°, the cells were stained with an FITC-conjugated anti-mouse CD8a antibody and a phycoerythrin (PE) -conjugated anti-mouse IgG1 antibody (BD PharMingen). The proportion of HBsAg-specific cells was measured by flow cytometry on a FACSCanto II instrument (Becton Dickinson Immunocytometry Systems, Mountain View, CA).

Cytotoxicity assay

The cytolytic activity of HBsAg-specific CTLs was assessed using a fluorescence-based dye, 5-(and 6-)carboxyfluorescein diacetate succinimidyl ester (CFSE) as described previously.[17] Target cells (P815 or P815preS1) were labelled with CFSE as follows. The cells were suspended in PBS and diluted to 1×10^6/ml. For sensitive targets, 0.5 μl of CFSE stock solution (5 mM) was added to 1 ml of cell suspension and the mixture was incubated for 4 min at room temperature. For control targets, 0.5 μl of diluted CFSE solution (100 μM) was used for labelling, in a similar fashion. Labelled targets and various numbers of effector cells were added in a final volume of 200 μl to each well of 96-well round-bottom plates and incubated for 6 hr at 37°. After incubation, sensitive target cells were mixed with control target cells in one tube with PBS containing 1% fetal calf serum and 0.1% sodium azide. Mixed cells were washed once, suspended in 4% paraformaldehyde, and then stored at 4° in the dark before flow cytometric analysis, which was performed on a FACSCan-

to II instrument (Becton Dickinson Immunocytometry Systems). All samples were assayed in duplicate and the mean percentage of specific lysis was calculated as follows: % specific lysis = [(number of sensitive target cells in the control sample – number of sensitive target cells in the test sample)/number of sensitive target cells in the control sample] × 100. The control sample consisted of target cells incubated without added effector cells, whereas the test sample consisted of target cells incubated with added effector cells.

Flow cytometric analysis of splenocytes

Splenocytes were isolated from the immunized mice as described previously.[18] Cell viability and cell number were assessed using a trypan blue exclusion assay. For flow cytometry, 2×10^5 splenocytes were stained with labelled antibodies using a standard protocol. The following antibodies were used: PE-Cy7-labelled anti-mouse CD8 mAb, clone 53-6.7 (eBioscience, San Diego, CA); PE-Cy7-labelled anti-mouse CD11b mAb (clone M1/70; eBioscience); VioBlue-labelled anti-mouse CD11c mAb (clone N418; Miltenyi Biotec GmbH, Bergisch Gladbach, Germany), FITC-labelled anti-mouse CD86 mAb (clone 24F; BD Biosciences); FITC-labelled anti-mouse Ly-6G mAb (clone RB6-8C5; BD Biosciences); PE-labelled anti-mouse CD80 mAb (clone BB1; BD Biosciences); PE-labelled anti-mouse Ly-6c mAb (clone AL-21; BD Biosciences); PE-labelled anti-mouse CD40 mAb (clone FKG45.5; Miltenyi Biotec); and PE-labelled anti-mouse Foxp3 mAb (clone FJK-16s; Biosciences). Samples were acquired on a flow cytometer and data analysis was performed using FACSDIVA software (BD Biosciences).

Real-time reverse transcription-PCR

Total RNA was isolated and transcribed into complementary DNA (cDNA) using an RNeasy Mini Kit (QIAGEN GmbH, Hilden, Germany) and a high-capacity cDNA transcription kit (Applied Biosystems, Foster City, CA). The resulting cDNA was used as a template for real-time PCR along with primer-probe sets for IDO, interleukin-2 (IL-2), IL-4, IL-6, IL-12b and 18S rRNA (TaqMan Gene Expression Assays; Applied Biosystems) and TaqMan universal PCR master mix (Applied Biosystems) according to the manufacturer's instructions (Applied Biosystems). The 18S rRNA was used as an internal control. Real-time PCR was carried out using a Light-Cycler 480 system (Roche Diagnostic Systems, Basel, Switzerland).

Isolation of $CD8^+$ and $CD11b^+$ cells

Splenocytes were sorted into $CD8^+$ or $CD11b^+$ cells using magnetic beads conjugated with an anti-CD8a or anti-CD11b antibody (Miltenyi Biotec GmbH) as described in previous reports.[19,20] The magnetically labelled cells were purified using a quadroMACS system (Miltenyi Biotec GmbH).

HBsAg-specific CTL proliferation assays

Isolated $CD11b^+$ and $CD11b^-$ cells were co-cultured with an HBsAg-specific CTL clone (6C2) in a CFSE-based proliferation assay.[21] The 6C2 cells were labelled with CFSE as previously described.[21] The CFSE-labelled cells were co-cultured with the purified $CD11b^+$ or $CD11b^-$ cells in 96-well plates at the cell-count ratios of 1 : 2 and 1 : 5 for the 6C2/$CD11b^+$ and the 6C2/$CD11b^-$ combinations, respectively, for 5 days at 37° in a 5% CO_2 atmosphere. To induce proliferation, the 6C2 cells were stimulated with irradiated P815PreS1 cells.

Statistics

Values were calculated as the mean ± SEM. Differences between experimental and control groups were analysed using the Kruskal–Wallis test followed by Scheffe's *F*-test. Significance was assumed at $P < 0.05$.

Results

Induction of the Tc1 immune response and HBsAg-specific $CD8^+$ T cells in WT and IDO-KO mice

Our previous study demonstrated that α-GalCer-activated invariant NKT cells strongly increased the number of HBsAg-specific CTLs after immunization with HBsAg *in vivo*.[5] Therefore, in the present study, we used α-GalCer as an adjuvant to enhance the HBsAg-specific immune response. To determine whether IDO contributes to the development of the HBsAg-specific immune response, WT and IDO-KO mice were immunized with HBsAg and α-GalCer intraperitoneally. As shown in Fig. 1(a), IDO-KO mice mounted strong Tc1 cellular responses against HBsAg, as indicated by the significant expansion of IFN-γ-producing cells in response to *ex vivo* re-stimulation with HBsAg peptide 28–39. Next, we examined CTL frequencies in the spleen using recombinant soluble fusion protein H-$2L^d$:Ig, which can be used to stain $CD8^+$ T cells that recognize the H-$2L^d$-bound HBsAg peptide $S_{28–39}$ (Fig. 1b,c). α-GalCer enhanced the numbers of WT as well as IDO-KO HBsAg-specific $CD8^+$ T cells. However, the induction of HBsAg-specific $CD8^+$ T cells was enhanced more strongly for the IDO-KO subset. Moreover, we examined the HBsAg-specific lysis caused by $CD8^+$ T cells from immunized WT and IDO-KO mice *ex vivo* (Fig. 1d). After immunization of mice with the HBsAg-α-GalCer combination, the HBsAg-specific lysis in $CD8^+$ T cells isolated from the IDO-KO mice was significantly enhanced compared with that induced by the WT cells.

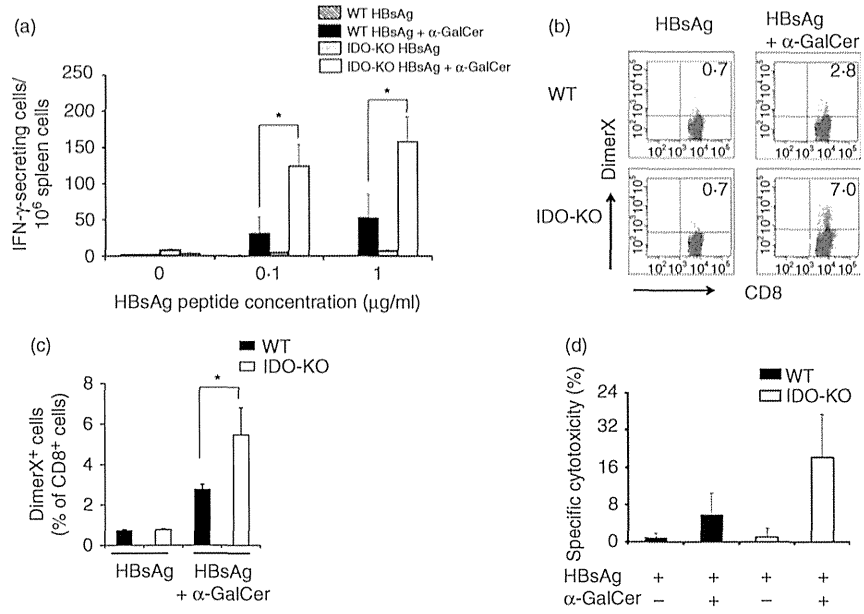

Figure 1. The induction of an hepatitis B virus surface antigen (HBsAg) S_{28-39}-specific T cytotoxic type 1 response and $CD8^+$ T cells in wild-type (WT) and indoleamine 2,3-dioxygenase knockout (IDO-KO) mice immunized with HBsAg alone or in combination with α-galactosylceramide (α-GalCer). Splenocytes were isolated from the animals 7 days after the immunization. (a) These cells were stimulated *ex vivo* with the HBsAg S_{28-39} peptide and monitored for interferon-γ (IFN-γ)-secreting cells by means of an ELISPOT assay. Results are shown as mean ± SEM (four or five mice/group) for three independent experiments. (b) Induction of HBsAg-specific $CD8^+$ T cells was assessed by flow cytometric analysis using fluorescent dimeric H-$2L^d$-HBsAg S_{28-39} complexes (DimerX). FACS profiles are shown for WT and IDO-KO mice immunized with either HBsAg or HBsAg plus α-GalCer. (c) Quantitative data on the frequency of dimeric H-$2L^d$-HBsAg-positive cell populations (mean ± SEM, $n = 4$). (d) Isolated effector cells ($CD8^+$ T cells) from WT and IDO-KO mice immunized with HBsAg and α-GalCer were incubated for 4 hr with CFSE-labelled target cells (preS1-transfected P815 cells) at an effector to target cell ratio of 20 : 1. The percentage of specific cytotoxicity was calculated by subtracting the percentage of P815 cells (HBsAg-negative) effector cell cytotoxicity from that for the preS1-transfected P815 cells (HBsAg-positive). Spontaneous release was always < 20% of the total. Each data point and error bar represents the mean and SEM, respectively, of results for triplicate samples. *Statistically significant differences.

Comparison of DC functions between WT and IDO-KO mice

Since α-GalCer can induce proliferation of the antigen-specific T cells via the activation of dendritic cells ($CD11c^+$ cells), we analysed dendritic cells from WT and IDO-KO mice immunized with HBsAg plus α-GalCer.[22] α-GalCer can up-regulate the expression of co-stimulatory molecules such as CD40, CD80 and CD86 in $CD11c^+$ cells (Fig. 2). Although the expression of these molecules on dendritic cells was enhanced bythe immunization with the HBsAg–α-GalCer combination, there was no difference between WT and IDO-KO mice.

Regulatory T cells and myeloid derived suppressor cells are stimulated by immunization with HBsAg and α-GalCer

Previous reports demonstrated that IDO was involved in the induction of regulatory T (Treg) cells.[23,24] We therefore examined the proliferation of Treg cells in WT and IDO-KO mice after inoculation with HBsAg and α-GalCer. Flow cytometry analysis revealed that the percentage of Treg cells in the spleen of WT and IDO-KO mice increased equally on day 7 after the immunization (Fig. 3a). The number of Treg cells did not decrease in IDO-KO mice after the HBsAg plus α-GalCer immunization in the present model. Myeloid derived suppressor cells (MDSCs) are identified by the expression of IDO, and were counted using flow cytometry. MDSCs are broadly defined as $CD11b^+$ $Ly6G^+$ mononuclear cells. The administration of HBsAg with α-GalCer expanded the MDSC population in WT and IDO-KO mice (Fig. 3b). This increase in MDSC frequency among spleen cells was observed 7 hr after the immunization, and was similar in both WT and IDO-KO mice.

IDO and cytokine production by WT and IDO-KO splenocytes in response to the intraperitoneal injection of HBsAg plus α-GalCer

Next, we examined whether the expression of IDO in the spleen is enhanced after the intraperitoneal adminis-

tration of the HBsAg–α-GalCer combination. This immunization promptly induced IDO expression in the spleen (Fig. 4a). Previous studies demonstrated that several cytokines play critical roles in the activation and proliferation of antigen-specific CTLs.[25,26] Accordingly, we measured mRNA levels for IL-2, IL-4, IL-6, IL-12b and IFN-γ in whole spleens from WT and IDO-KO mice after the co-administration of HBsAg and α-GalCer (Fig. 4b). The expression of IL-2, IL-4, IL-6 and IL-12b in the spleen of WT and IDO-KO mice was enhanced at 7 hr after the co-administration. In IDO-KO mice, however, compared with WT mice, the expression of IL-2 was significantly increased at 24 and 72 hr after the co-administration. Interleukin-12b expression in IDO-KO mice was also increased at 24 hr after the co-immunization with HBsAg and α-GalCer. These data indicate that after the co-administration, the enhancement of IL-2 and IL-12b expression persisted for longer in the spleen of the IDO-KO mice.

Induction and function of IDO in CD11b$^+$ cells after the immunization of mice with HBsAg and α-GalCer

As shown in Fig. 4(a), the expression of IDO mRNA was strongly enhanced at 7 hr after the administration of HBsAg and α-GalCer. Moreover, the number of CD11b$^+$ Ly6G$^+$ cells (MDSCs) in the spleen also increased at 7 hr after the immunization (Fig. 3b). For this reason, we examined the expression of IDO in CD11b$^+$ cells and CD11b$^-$ cells after the immunization of mice with HBsAg and α-GalCer. As a result of the immunization, the expression of IDO mRNA in CD11b$^+$ cells significantly increased compared with that in CD11b$^-$ cells (Fig. 5a). IDO was predominantly induced in CD11b$^+$ cells from the spleen. Next, we examined the function of CD11b$^+$ cells in HBsAg-specific T-cell proliferation in WT and IDO-KO mice. 6C2 cells are HBsAg-specific CTL clones. We labelled these CTLs with CFSE and stimulated them using irradiated P815PreS1 cells either in the presence or in the absence of CD11b$^+$ cells from WT or IDO-KO mice (Fig. 5c). 6C2 cell proliferation was evaluated by CFSE dilution. For WT mice, the presence of CD11b$^+$ cells inhibited the proliferation of the HBsAg-specific CTLs 6C2 in response to the target cells, after immunization of mice with HBsAg and α-GalCer. In contrast, enhanced cell proliferation was observed when IDO-KO cells were used under similar conditions. In addition, the expression of IL-12b in CD11b$^+$ cells from immunized WT and IDO-KO mice increased compared with that in the CD11b$^-$ subset (Fig. 5b). The enhanced IL-12b production by IDO-KO CD11b$^+$ cells may have contributed to the 6C2 cell proliferation in response to the P815PreS1 cells.

Effect of 1-MT on the induction of the HBsAg-specific immune response

1-Methyl-D-tryptophan is a potent inhibitor of IDO, and hence we used this agent to verify our finding. The WT mice were given 1-MT orally at either 0 or 5 mg/ml in drinking water 2 days before the immunization to 7 days after the immunization. ELISPOT analysis revealed that the HBsAg peptide S_{28-39}-specific Tc1 response in WT mice treated with 1-MT was significantly stronger compared with the untreated mice (Fig. 6a). The induction of HBsAg-specific CD8$^+$ T cells was enhanced by treatment with 1-MT (Fig. 6b,c). These data indicate that the inhibition of IDO activity leads to the enhancement of an HBsAg-specific Tc1 response after immunization with HBsAg and α-GalCer.

Discussion

In the present study, we demonstrated that inhibition of IDO activity enhances the HBsAg-specific Tc1 response and induction of CTLs after immunization with HBsAg and α-GalCer. The expression of IL-2 and IL-12b, which are critical cytokines for inducing the antigen-specific Tc1 response, increases in IDO knockout mice after immunization with HBsAg and α-GalCer. Moreover, CD11b$^+$ splenocytes up-regulate their expression of IDO and suppress the proliferation of HBsAg-specific CTLs after immunization of mice with HBsAg and α-GalCer treatment. Hence, the α-GalCer-induced increase of IDO expression reduced the antigen-specific Tc1 immunity. On the other hand, inhibition of IDO expression after the HBsAg plus α-GalCer immunization strongly enhanced the HBsAg-specific cellular immune response.

Previously, we demonstrated that during immunization with HBsAg, α-GalCer works as an adjuvant and enhances the induction of an HBsAg-specific CTL response *in vivo*.[5] It appears that IL-2 and CD40–CD40 ligand interactions are involved in the enhancement of CTL induction caused by α-GalCer through NKT cell activation. On the other hand, α-GalCer enhances the activity of IDO in mice.[13] IDO catalyses the conversion of the essential amino acid L-tryptophan to L-kynurenine and has been identified as an enzyme that has powerful immunomodulatory effects. Furthermore, metabolites of the L-kynurenine pathway have been shown to act as immunosuppressive molecules in the tissue microenvironment.[27,28] IDO and the L-tryptophan pathway play critical roles in the generation of immune tolerance against foreign antigens in tissue microenvironments. In the present study, IDO expression in splenocytes also increased after HBsAg and α-GalCer administration (Fig. 5a). As shown in Fig. 1(a), the intraperitoneal injection of HBsAg and α-GalCer increased the HBsAg-specific Tc1 immune response, and this Tc1 response was enhanced more

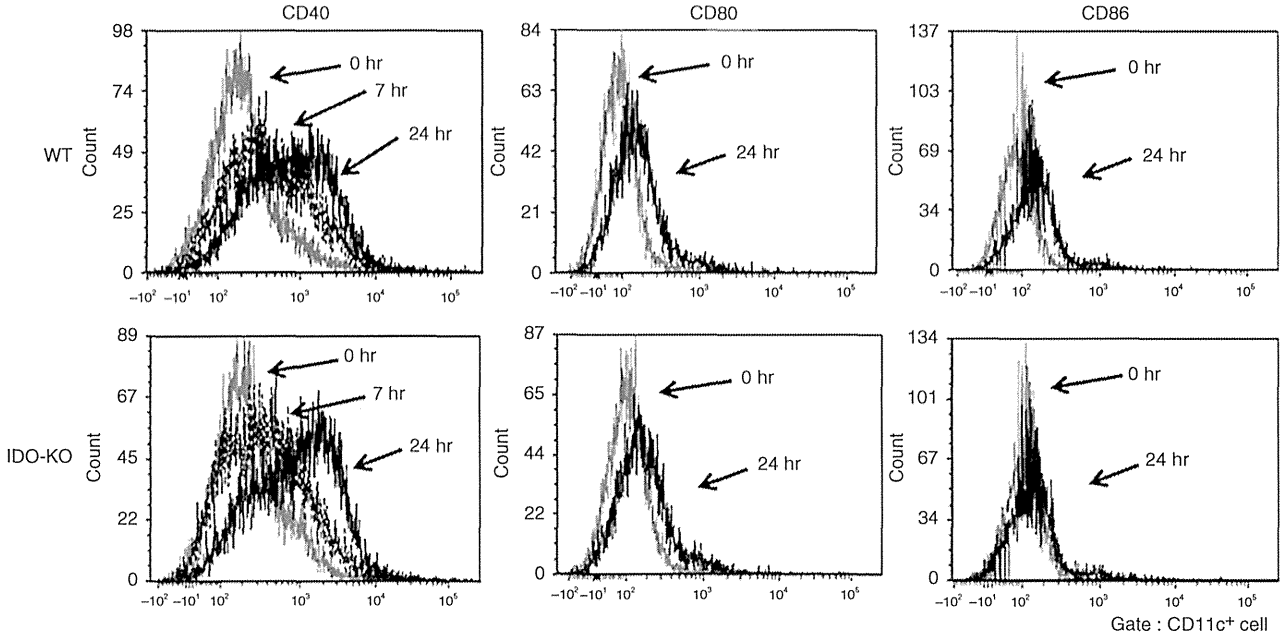

Figure 2. The expression of co-stimulatory molecules on dendritic cells from wild-type (WT) and indoleamine 2,3-dioxygenase knockout (IDO-KO) mice. At 0, 7 and 24 hr after the inoculation with hepatitis B virus surface antigen (HBsAg) and α-galactosylceramide (α-GalCer) (intraperitoneal injection), the expression of CD40, CD80 and CD86 on splenic $CD11c^+$ cells was analysed using flow cytometry. The data represent three independent identical experiments.

strongly in IDO-KO mice compared with WT mice. Moreover, the number of $CD8^+$ T cells that can specifically recognize HBsAg and cause HBsAg-mediated lysis also increased in IDO-KO mice *ex vivo* (Fig. 1b–d). These results suggest that the absence of IDO activity significantly enhances the HBsAg-specific Tc1 immune response after the immunization with HBsAg and α-GalCer. 1-MT is a competitive inhibitor of the IDO activity. As shown in Fig. 6, the administration of HBsAg, α-GalCer and 1-MT also enhanced both the HBsAg-specific Tc1 response and the induction of HBsAg-specific $CD8^+$ T cells (Fig. 6a–c). However, the HBsAg-specific Tc1 response in the mice treated with HBsAg, α-GalCer and 1-MT was weak compared with that in the IDO-KO mice treated with HBsAg and α-GalCer. A previous report indicated that the L-kynurenine level in IDO-KO mice was lower than that in 1-MT-treated mice during *Toxoplasma gondii* infection *in vivo*.[29] Our previous study also indicated a difference in proliferation of splenocytes and viral replication between IDO-KO mice and 1-MT-treated mice during LP-BM5 murine leukaemia virus infection.[9] We assumed that complete local depletion of L-tryptophan is critical for the immune system, and the oral administration of 1-MT may fail to fully suppress local IDO activity. Several reports have demonstrated that the enhancement of the immune response by α-GalCer involves an up-regulation of co-stimulatory molecules such as CD80, CD86 and CD40.[22,30] In the present work, although α-GalCer enhanced the expression of CD40 and CD86 in $CD11c^+$ cells, this effect was similar in WT and IDO-KO mice (Fig. 2). Real-time PCR analysis revealed that the expression of IL-2 and IL-12b was elevated at 24 and 72 hr after the HBsAg plus α-GalCer immunization in IDO-KO mice compared with that in WT mice (Fig. 4b). The expression of IL-2, IL-4, IL-6 and IL-12b increased at 7 hr after administration, and promptly decreased afterwards in WT mice. On the other hand, in IDO-KO mice, the enhancement of IL-2 and IL-12b expression was maintained between 24 and 72 hr after the immunization with HBsAg and α-GalCer. The persistence of the elevated expression of IL-2 and IL-12b in IDO-KO mice may play a role in the enhancement of the HBsAg-specific Tc1 immune response induced by HBsAg and α-GalCer in combination.

IDO is strongly activated by IFN-γ or pro-inflammatory cytokines in macrophages/monocytes. As shown in Fig. 5(a), among splenocytes, the immunization of mice with HBsAg and α-GalCer induced IDO activity almost exclusively in $CD11b^+$ cells. No enhancement of IDO expression was observed in $CD11b^-$ cells. In addition, $CD11b^+$ cells from HBsAg-plus-α-GalCer-immunized WT mice reduced the proliferation of HBsAg-specific CTLs when the latter were stimulated with the specific antigen (Fig. 5c). In contrast, $CD11b^+$ cells from HBsAg-plus-α-GalCer-immunized IDO-KO mice facilitated the proliferation of HBsAg-specific CTLs. These results indicate that IDO-deficient $CD11b^+$ cells treated with α-GalCer have a strong ability to enhance proliferation of HBsAg-specific

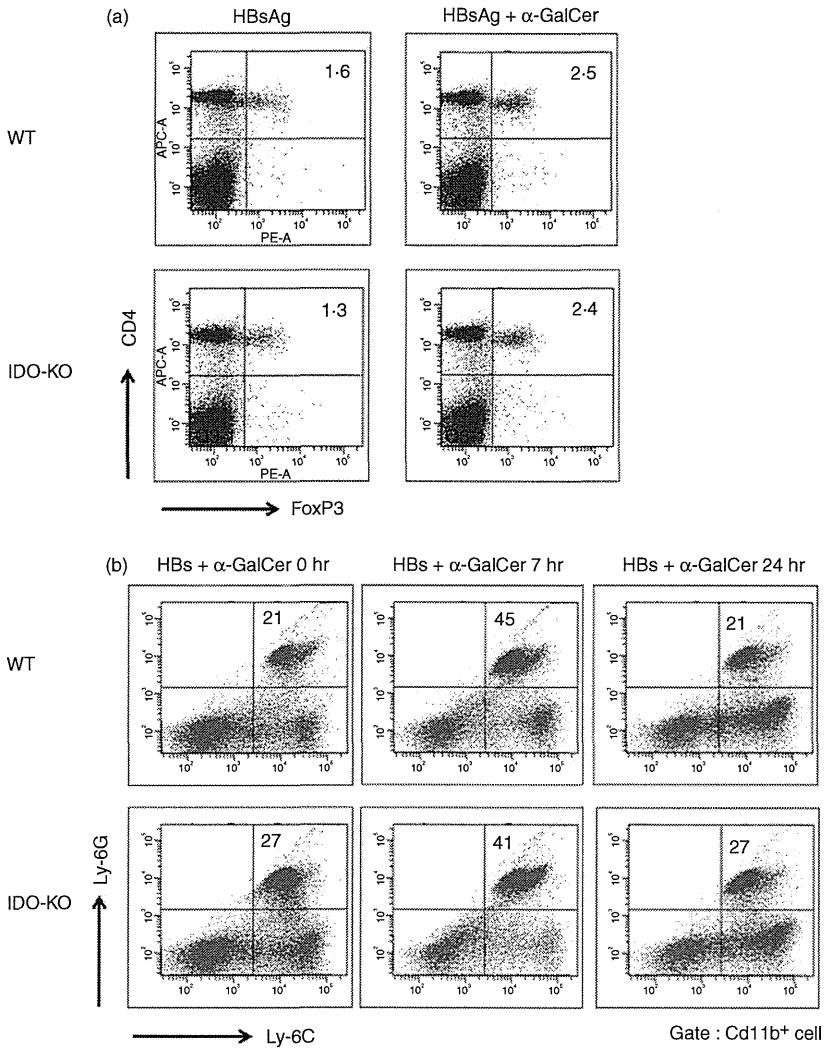

Figure 3. The induction of regulatory T cells and myeloid derived suppressor cells (MDSCs) in wild-type (WT) and indoleamine 2,3-dioxygenase knockout (IDO-KO) mice immunized with hepatitis B virus surface antigen (HBsAg) and α-galactosylceramide (α-GalCer). (a) Flow cytometric analysis of intracellular FoxP3 expression in $CD4^+$ T cells obtained from WT and IDO-KO mice on day 7 after inoculation with HBsAg and α-GalCer. The data represent three independent identical experiments. (b) Flow cytometric analysis of surface Ly-6G and Ly-6C expression on $CD11b^+$ cells from WT and IDO-KO mice at 7 and 24 hr after inoculation with HBsAg and α-GalCer. The data represent three independent identical experiments.

CTLs. The expression of IL-12b in $CD11b^+$ cells was increased at 7 hr after the immunization with HBsAg plus α-GalCer (Fig. 5b). Moreover, the $CD11b^+$ fraction included the $CD11b^+$ $CD11c^+$ cells, and the expression of co-stimulatory molecules on $CD11c^+$ cells increased after the immunization (Fig. 2). Hence, the $CD11b^+$ cells from the IDO-KO mice immunized with HBsAg and α-GalCer may enhance the proliferation of HBsAg-specific CTLs via an increase in IL-12b production and co-stimulatory molecule expression. The intraperitoneal administration of HBsAg and α-GalCer increased the proportion of $CD11b^+$ $Ly6G^+$ cells in the spleen (Fig. 3b). $CD11b^+$ $Ly6G^+$ cells are known as MDSCs and induce the expression of IDO, which inhibits the immune response.[31] Hence, the immunization with HBsAg and α-GalCer increases the proportion of $CD11b^+$ $Ly6G^+$ cells in the spleen as well as the number of IDO-producing cells and thereby inhibits the induction of an HBsAg-specific immune response. Although the immunization with HBsAg and α-GalCer also increased the proportion of $CD11b^+$ $Ly6G^+$ cells in IDO-KO mice, these cells cannot up-regulate IDO and inhibit the HBsAg-specific immune response. Several reports demonstrated that IDO stimulates Treg cells and suppresses the immune response.[23,24] On the other hand, there was no difference in the percentage of Treg cells between the non-treated group and the 1-MT-treated group in a rheumatoid arthritis mouse model.[32] Our previous report also demonstrated that the expression of FoxP3 mRNA in WT and IDO-KO mice was up-regulated after LP-BM5 murine leukaemia virus infection and there was no difference in FoxP3 mRNA expression.[9] The inoculation with HBsAg and α-GalCer injection increased the proportion of $CD4^+$ $FoxP3^+$ T cells in the spleen (Fig. 3a), but there was no difference in Treg cell number between WT mice and IDO-KO mice. Therefore, in this study, Treg cells do not appear to be involved in the HBsAg-specific immune response following immunization with HBsAg plus α-GalCer.

A recent study evaluated the effect of IDO on the humoral immune response, and they demonstrated that inhibition of IDO by the administration with 1-MT at

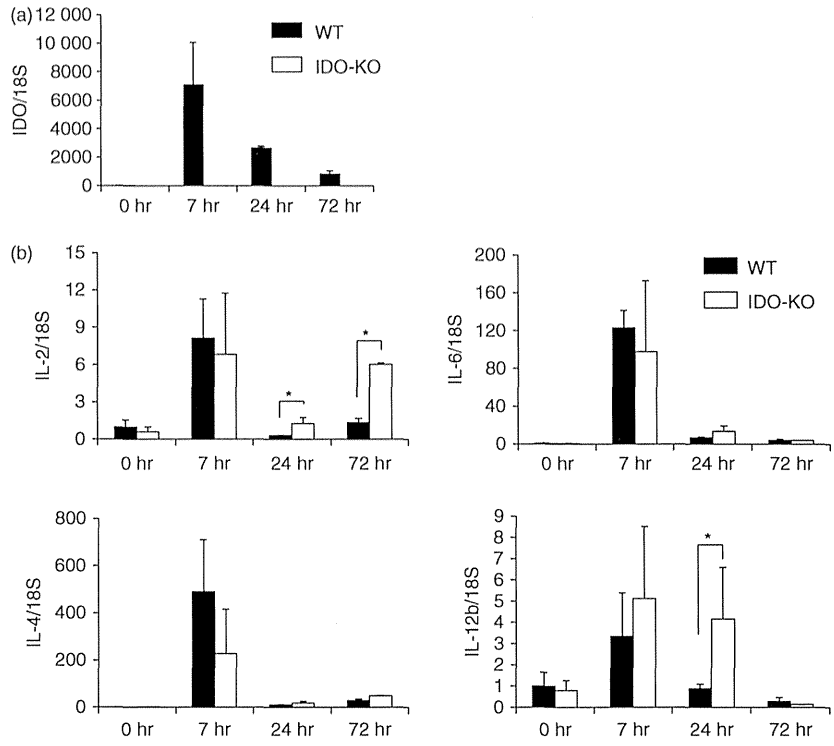

Figure 4. Indoleamine 2,3-dioxygenase knockout (IDO) and cytokine production by splenocytes from wild-type (WT) and IDO knockout (IDO-KO) mice in response to an intraperitoneal injection with hepatitis B virus surface antigen (HBsAg) and α-galactosylceramide (α-GalCer). In all graphs, the *y*-axis shows arbitrary units. (a) The relative expression levels of IDO mRNA in the spleen of WT and IDO-KO mice were measured using quantitative real-time RT-PCR. The results were normalized for the expression of 18S rRNA. Each value is shown as mean (SEM) for three mice. (b) The relative expression levels of interleukin-2 (IL-2), IL-4, IL-6 and IL-12b mRNA in the spleen of WT and IDO-KO mice were measured using quantitative real-time RT-PCR. The results were normalized for the expression of 18S rRNA. Each data point and error bar represents the mean and SEM, respectively, of data from triplicate samples. *Statistically significant differences.

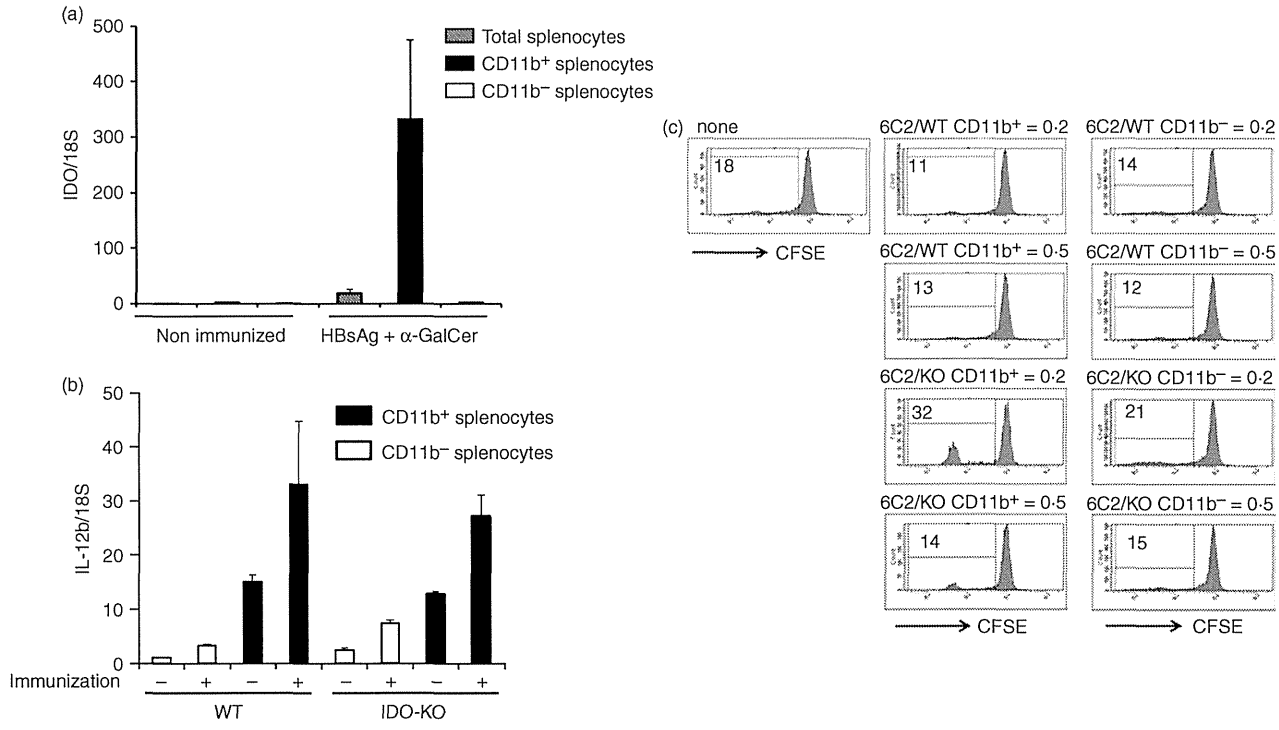

Figure 5. Induction and function of indoleamine 2,3-dioxygenase (IDO) in CD11b$^+$ cells from wild-type (WT) and IDO knockout (IDO-KO) mice after the inoculation with hepatitis B virus surface antigen (HBsAg) and α-galactosylceramide (α-GalCer). (a, b) Splenic CD11b$^+$ and CD11b$^-$ cells were purified using immunomagnetic separation 7 hr after the inoculation and used to prepare total mRNA. The expression of IDO and interleukin-12b (IL-12b) mRNA was analysed using real-time RT-PCR. Results were normalized for the expression of 18S rRNA. (c) CFSE-labelled 6C2 cells were co-cultured with the purified CD11b$^+$ or CD11b$^-$ cells in 96-well plates at a cell-count ratio of 1 : 2 or 1 : 5 for 6C2/ myeloid derived suppressor cell or 6C2/control combination, respectively, for 5 days. To induce proliferation, the 6C2 cells were stimulated with irradiated P815PreS1 cells.

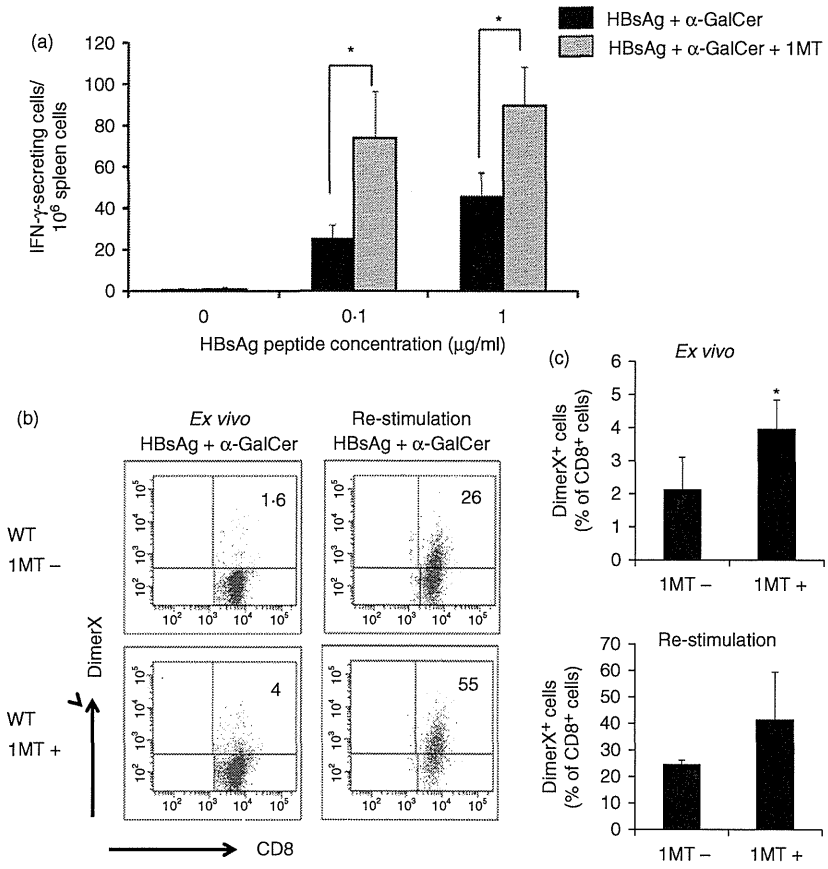

Figure 6. The effects of 1-methyl-D-L-tryptophan (1-MT) on the induction of an hepatitis B virus surface antigen (HBsAg) -specific immune response. (a) Wild-type (WT) mice received 1-MT orally at a dose of either 0 or 5 mg/ml in drinking water 2 days before the immunization to 7 days after the immunization. Splenocytes from these mice were isolated 7 days after the immunization. These cells were stimulated *ex vivo* with the HBsAg S_{28-39} peptide and monitored for interferon-γ-secreting cells by means of an ELISPOT assay. The results are shown as mean ± SEM (four or five mice/group) for three independent experiments. (b) Induction of HBsAg-specific $CD8^+$ T cells was assessed by means of flow cytometric analysis using fluorescent dimeric H-$2L^d$-HBsAg S_{28-39} complexes (DimerX). FACS profiles are shown for WT mice and for 1-MT-treated WT mice after the inoculation with HBsAg and α-galactosylceramide (α-GalCer). (c) Quantitative data on the frequency of dimeric H-$2L^d$-HBsAg-positive cell populations (mean ± SEM, $n = 4$). *Statistically significant differences.

the time of vaccination decreased the serum anti-HBs antibody level after HBsAg vaccination.[33] Another report showed that 1-MT inhibit the B cells' ability to differentiate into autoantibody-secreting cells and improve autoimmune arthritis.[34] These studies indicated that 1-MT inhibits the humoral immune response. The enhancement of HBs-antibody induction is critical to prevent HBV infection. On the other hand, the induction of a cellular immune response to HBV antigen is pivotal to the complete elimination of HBV during chronic infection.[35] Enhancement of the induction of HBsAg-specific CTLs may be helpful in developing strategies to clear HBV in patients with chronic hepatitis.

We can conclude that the inhibition of IDO activity significantly enhanced the induction of HBsAg-specific CTLs following immunization with HBsAg and α-GalCer. The addition of α-GalCer enhances IDO activity, which inhibits the activation and proliferation of antigen-specific CTLs. Hence, abrogation of the α-GalCer-mediated enhancement of IDO activity makes the HBsAg-specific Tc1 response much more powerful. These results lead to strategies for improving the induction of HBsAg-specific CTLs.

Acknowledgements

This work was supported by the Grant-in-Aid for Exploratory Research (24659361) from the Ministry of Education, Culture, Sports, Science and Technology of Japan.

Disclosures

The authors have no financial or commercial conflict of interest.

References

1 Guidotti LG. The role of cytotoxic T cells and cytokines in the control of hepatitis B virus infection. *Vaccine* 2002; **20**(Suppl 4):A80–2.
2 Shan L, Deng K, Shroff NS *et al.* Stimulation of HIV-1-specific cytolytic T lymphocytes facilitates elimination of latent viral reservoir after virus reactivation. *Immunity* 2012; **36**:491–501.
3 Ito H, Seishima M. Regulation of the induction and function of cytotoxic T lymphocytes by natural killer T cell. *J Biomed Biotechnol* 2010; **2010**:641757.
4 Kim D, Hung CF, Wu TC, Park YM. DNA vaccine with α-galactosylceramide at prime phase enhances anti-tumor immunity after boosting with antigen-expressing dendritic cells. *Vaccine* 2010; **28**:7297–305.
5 Ito H, Ando K, Ishikawa T *et al.* Role of $V\alpha14^+$ NKT cells in the development of hepatitis B virus-specific CTL: activation of $V\alpha14^+$ NKT cells promotes the breakage of CTL tolerance. *Int Immunol* 2008; **20**:869–79.
6 Munn DH, Shafizadeh E, Attwood JT, Bondarev I, Pashine A, Mellor AL. Inhibition of T cell proliferation by macrophage tryptophan catabolism. *J Exp Med* 1999; **189**:1363–72.
7 Mellor AL, Munn DH. Tryptophan catabolism and T-cell tolerance: immunosuppression by starvation? *Immunol Today* 1999; **20**:469–73.
8 Fujigaki S, Saito K, Sekikawa K *et al.* Lipopolysaccharide induction of indoleamine 2,3-dioxygenase is mediated dominantly by an IFN-γ-independent mechanism. *Eur J Immunol* 2001; **31**:2313–8.
9 Hoshi M, Saito K, Hara A *et al.* The absence of IDO upregulates type I IFN production, resulting in suppression of viral replication in the retrovirus-infected mouse. *J Immunol* 2010; **185**:3305–12.

10 Hoshi M, Matsumoto K, Ito H *et al.* L-Tryptophan–kynurenine pathway metabolites regulate type I IFNs of acute viral myocarditis in mice. *J Immunol* 2012; **188**:3980–7.

11 Fallarino F, Grohmann U, Hwang KW *et al.* Modulation of tryptophan catabolism by regulatory T cells. *Nat Immunol* 2003; **4**:1206–12.

12 Grohmann U, Fallarino F, Bianchi R *et al.* A defect in tryptophan catabolism impairs tolerance in nonobese diabetic mice. *J Exp Med* 2003; **198**:153–60.

13 Ito H, Hoshi M, Ohtaki H *et al.* Ability of IDO to attenuate liver injury in α-galactosylceramide-induced hepatitis model. *J Immunol* 2010; **185**:4554–60.

14 Ando K, Guidotti LG, Wirth S *et al.* Class I-restricted cytotoxic T lymphocytes are directly cytopathic for their target cells *in vivo*. *J Immunol* 1994; **152**:3245–53.

15 Ando K, Guidotti LG, Cerny A, Ishikawa T, Chisari FV. CTL access to tissue antigen is restricted *in vivo*. *J Immunol* 1994; **153**:482–8.

16 Kasahara S, Ando K, Saito K *et al.* Lack of tumor necrosis factor α induces impaired proliferation of hepatitis B virus-specific cytotoxic T lymphocytes. *J Virol* 2003; **77**:2469–76.

17 Nakagawa Y, Watari E, Shimizu M, Takahashi H. One-step simple assay to determine antigen-specific cytotoxic activities by single-color flow cytometry. *Biomed Res* 2011; **32**:159–66.

18 Ito H, Ando K, Nakayama T *et al.* Role of Vα14 NKT cells in the development of impaired liver regeneration *in vivo*. *Hepatology* 2003; **38**:1116–24.

19 Ito H, Ando K, Ishikawa T *et al.* Role of TNF-α produced by nonantigen-specific cells in a fulminant hepatitis mouse model. *J Immunol* 2009; **182**:391–7.

20 Ohtaki H, Ito H, Hoshi M *et al.* High susceptibility to lipopolysaccharide-induced lethal shock in encephalomyocarditis virus-infected mice. *Sci Rep* 2012; **2**:367.

21 Mandapathil M, Lang S, Gorelik E, Whiteside TL. Isolation of functional human regulatory T cells (Treg) from the peripheral blood based on the CD39 expression. *J Immunol Methods* 2009; **346**:55–63.

22 Joyee AG, Uzonna J, Yang X. Invariant NKT cells preferentially modulate the function of $CD8\alpha^+$ dendritic cell subset in inducing type 1 immunity against infection. *J Immunol* 2010; **184**:2095–106.

23 Yan Y, Zhang GX, Gran B *et al.* IDO upregulates regulatory T cells via tryptophan catabolite and suppresses encephalitogenic T cell responses in experimental autoimmune encephalomyelitis. *J Immunol* 2010; **185**:5953–61.

24 Matteoli G, Mazzini E, Iliev ID *et al.* Gut $CD103^+$ dendritic cells express indoleamine 2,3-dioxygenase which influences T regulatory/T effector cell balance and oral tolerance induction. *Gut* 2010; **59**:595–604.

25 Bachmann MF, Schorle H, Kuhn R *et al.* Antiviral immune responses in mice deficient for both interleukin-2 and interleukin-4. *J Virol* 1995; **69**:4842–6.

26 Widmer MB, Grabstein KH. Regulation of cytolytic T-lymphocyte generation by B-cell stimulatory factor. *Nature* 1987; **326**:795–8.

27 Terness P, Bauer TM, Rose L *et al.* Inhibition of allogeneic T cell proliferation by indoleamine 2,3-dioxygenase-expressing dendritic cells: mediation of suppression by tryptophan metabolites. *J Exp Med* 2002; **196**:447–57.

28 Fallarino F, Grohmann U, Puccetti P. Indoleamine 2,3-dioxygenase: from catalyst to signaling function. *Eur J Immunol* 2012; **42**:1932–7.

29 Murakami Y, Hoshi M, Hara A *et al.* Inhibition of increased indoleamine 2,3-dioxygenase activity attenuates *Toxoplasma gondii* replication in the lung during acute infection. *Cytokine* 2012; **59**:245–51.

30 Taraban VY, Martin S, Attfield KE *et al.* Invariant NKT cells promote $CD8^+$ cytotoxic T cell responses by inducing CD70 expression on dendritic cells. *J Immunol* 2008; **180**:4615–20.

31 Yu J, Du W, Yan F *et al.* Myeloid-derived suppressor cells suppress antitumor immune responses through IDO expression and correlate with lymph node metastasis in patients with breast cancer. *J Immunol* 2013; **190**:3783–97.

32 Scott GN, DuHadaway J, Pigott E *et al.* The immunoregulatory enzyme IDO paradoxically drives B cell-mediated autoimmunity. *J Immunol* 2009; **182**:7509–17.

33 Eleftheriadis T, Sparopoulou T, Antoniadi G, Liakopoulos V, Stefanidis I, Galaktidou G. Suppression of humoral immune response to hepatitis B surface antigen vaccine in BALB/c mice by 1-methyl-tryptophan co-administration. *Daru* 2011; **19**:236–9.

34 Pigott E, Mandik-Nayak L. Addition of an indoleamine 2,3,-dioxygenase inhibitor to B cell-depletion therapy blocks autoreactive B cell activation and recurrence of arthritis in K/BxN mice. *Arthritis Rheum* 2012; **64**:2169–78.

35 Guidotti LG, Ishikawa T, Hobbs MV, Matzke B, Schreiber R, Chisari FV. Intracellular inactivation of the hepatitis B virus by cytotoxic T lymphocytes. *Immunity* 1996; **4**:25–36.

Biochimica et Biophysica Acta 1842 (2014) 1464–1471

Contents lists available at ScienceDirect

Biochimica et Biophysica Acta

journal homepage: www.elsevier.com/locate/bbadis

Kynurenine production mediated by indoleamine 2,3-dioxygenase aggravates liver injury in HBV-specific CTL-induced fulminant hepatitis

Hirofumi Ohtaki [a], Hiroyasu Ito [a,*], Kazuki Ando [a], Tetsuya Ishikawa [d], Masato Hoshi [a], Tatsuya Ando [a], Manabu Takamatsu [b], Akira Hara [b], Hisataka Moriwaki [c], Kuniaki Saito [e], Mitsuru Seishima [a]

[a] Department of Informative Clinical Medicine, Gifu University Graduate School of Medicine, 1-1 Yanagido, Gifu 501-1194, Japan
[b] Department of Pathology, Gifu University Graduate School of Medicine, 1-1 Yanagido, Gifu 501-1194, Japan
[c] First Department of Internal Medicine, Gifu University Graduate School of Medicine, 1-1 Yanagido, Gifu 501-1194, Japan
[d] Department of Medical Technology, Nagoya University School of Health Sciences, 1-20 Daikominami-1-chome, Higashi-ku, Nagoya, Aichi 461-8673, Japan
[e] Human Health Sciences, Graduate School of Medicine and Faculty of Medicine, Kyoto University, 53 Kawahara-cho, Shogoin, Sakyo, Kyoto 606-8507, Japan

ARTICLE INFO

Article history:
Received 24 December 2013
Received in revised form 11 April 2014
Accepted 14 April 2014
Available online 24 April 2014

Keywords:
Fulminant hepatitis
Hepatitis B virus
Indoleamine 2,3-dioxygenase
Kynurenine

ABSTRACT

Indoleamine 2,3-dioxygenase (IDO), an enzyme that is ubiquitously distributed in mammalian tissues and cells, converts tryptophan to kynurenine, and is also known as a key molecule that promotes apoptosis in lymphocytes and neurons. In this study, we established hepatitis B virus (HBV)-transgenic (Tg)/IDO-knockout (KO) mice and examined the influence of IDO in a murine fulminant hepatitis model induced by HBV-specific cytotoxic T lymphocytes (CTL). An increase of IDO expression in the livers of HBV-Tg/IDO-wild-type (WT) mice administered HBV-specific CTL was confirmed by real-time polymerase chain reaction, western blotting, and evaluating IDO activity. Plasma alanine aminotransferase (ALT) levels in HBV-Tg/IDO-KO mice after HBV-specific CTL injection significantly decreased compared with those in HBV-Tg/IDO-WT mice. An inhibitor of IDO, 1-methyl-D-tryptophan (1-MT), could also attenuated the observed liver injury induced by this HBV-specific CTL. The expression levels of cytokine and chemokine mRNAs in the livers of HBV-Tg/IDO-WT mice were higher than those in the livers of HBV-Tg/IDO-KO mice. The administration of kynurenine aggravated the liver injury in HBV-Tg/IDO-KO mice injected with HBV-specific CTL. Simultaneous injection of recombinant murine interferon (IFN-γ) and kynurenine also increased the ALT levels in HBV-Tg/IDO-KO mice. The liver injury induced by IFN-γ and kynurenine was improved in HBV-Tg/tumor necrosis factor-α-KO mice. *Conclusion*: Kynurenine and IFN-γ induced by the administration with HBV-specific CTL are cooperatively involved in the progression of liver injury in acute hepatitis model. Our results may lead to a new therapy for the acute liver injury caused by HBV infection.

1. Introduction

Fulminant hepatitis is a severe, rapidly progressive loss of hepatic function due to viral infection or other cause of inflammatory destruction of liver tissue [1]. Hepatitis B virus (HBV) infection can cause fulminant hepatitis; this disease has a high mortality rate despite intensive medical care and the implementation of the latest therapies, including liver transplantation. HBV is a non-lytic virus that does not cause direct cell damage [2]. Liver damage and viral clearance after HBV infection are thought to be mediated by the host cellular immune response to viral antigens. A fulminant hepatitis model has been examined in mice by using adoptive transfer of HBV-specific cytotoxic T lymphocytes (CTL) into HBV-transgenic (Tg) mice [3–5]. The mice develop a necroinflammatory liver disease that is histologically similar to acute viral hepatitis in humans. Various studies have been performed on viral clearance and liver diseases in HBV infection by using this murine fulminant hepatitis model [4,6,7].

Indoleamine 2,3-dioxygenase (IDO) is an enzyme that is ubiquitously distributed in mammalian tissues and cells; this enzyme converts tryptophan to *N*-formylkynurenine, which is further catabolized to kynurenine. IDO is induced via an IFN-γ dependent and/or an independent mechanism as well as other pro-inflammatory cytokines in the course of an inflammatory response in various cell types, including macrophages, fibroblasts, and epithelial cells [8,9]. Previously, we reported that IDO expression in hepatocytes is increased after HBV-specific CTL injection into HBV-Tg mice [7]. In this model, IFN-γ induced by the CTL injection was involved in the observed increase in the IDO expression on the liver, which is also reportedly up-regulated in hepatitis virus-infected woodchuck [10]. Thus, IDO expression in the liver is strongly increased in acute and fulminant viral hepatitis. Kynurenine and other tryptophan metabolites produced by IDO promote cell death and tissue injury [11]. On the other hand, immune-mediated diseases such as GVHD are improved by the activation of IDO [12].

* Corresponding author. Tel.: +81 58 230 6430; fax: +81 58 230 6431.
E-mail address: hito@gifu-u.ac.jp (H. Ito).

http://dx.doi.org/10.1016/j.bbadis.2014.04.015
0925-4439/

These findings indicate that IDO has conflicting function in tissue injury. The role of increased IDO expression is not defined clearly in the fulminant hepatitis model induced by HBV-specific CTL. In the present study, we established HBV-Tg/IDO-KO mice and examined the influence of induced IDO during acute liver injury caused by HBV-specific CTL.

2. Material and methods

2.1. Reagents

1-Methyl-D-tryptophan (1-MT) and L-kynurenine were purchased from Sigma-Aldrich (St. Louis, MO). Recombinant murine IFN-γ was purchased from Peprotech (Rocky Hill, NJ).

2.2. Mice

The HBV-Tg mouse lineage 107-5D (official designation Tg [Alb-1, HBV] Bri66; inbred B10.D2, H-2d), in which the HBV envelope coding region is under the control of the mouse albumin promoter, was provided by Dr. F. V. Chisari (Department of Molecular and Experimental Medicine, Scripps Research Institute, La Jolla, CA). IDO1 gene knockout (IDO-KO) mice on a C57BL/6J background were obtained from Jackson Laboratory (Bar Harbor, ME) and backcrossed to B10.D2 (H-2d). HBV-Tg/IDO-KO mice were produced by backcrossing IDO-KO mice with 107-5D. TNF-α-KO mice were produced by gene targeting as described previously [13] and backcrossed onto B10.D2 (H-2d). HBV-Tg/TNF-α-KO mice were produced by backcrossing TNF-α-KO mice with 107-5D. All animal procedures were conducted in accordance with the National Institutes of Health Guide for the Care and Use of Laboratory Animals, and guidelines for the care and use of animals established by the Animal Care and Use Committee of Gifu University.

2.3. Cell lines

P815 cells expressing HBV-preS1, 2, and S (P815preS1) were provided by Dr. F. V. Chisari. HBV-specific $CD8^+$ CTL clones were produced as described in a previous report [14]. The clones are H-2d restricted, and can recognize an epitope (IPQSLDSWWTSL) located between residues 28 and 39 of the hepatitis B surface antigen (HBsAg). The CTL were washed 5 d after a final stimulation with irradiated P815preS1 and then intravenously injected into HBV-Tg mice.

2.4. Fulminant hepatitis model and assessment of hepatocellular injury

HBV-specific $CD8^+$ CTL clones (1×10^6/mouse) were intravenously injected into HBV-Tg/IDO-WT, IDO-WT, HBV-Tg/IDO-KO, and IDO-KO mice. To monitor hepatocellular injury, plasma alanine aminotransferase (ALT) activity was measured using an automated clinical analyzer BM2250 (JEOL, Tokyo, Japan).

2.5. Histological examination

Histopathological examination of the liver was performed at 0 d and 2 d after CTL injection. The liver was fixed with 10% formalin in PBS for 48 h and then embedded in paraffin. Tissue sections were deparaffinized, stained with hematoxylin and eosin, and examined under light microscopy. TUNEL staining was performed using in situ apoptosis detection kit (Takara Bio, Shiga, Japan), according to the manufacturer's instructions. Necroinflammatory foci are defined as the existence of inflammatory cell infiltration and hepatocyte necrosis more than three, and inflammatory cell foci are defined as the existence of inflammatory cell more than ten in paraffin sections of the liver. The data are represented as the numerical value per area (1 mm^2).

2.6. Measurement of kynurenine

Kynurenine was measured using high-performance liquid chromatography (HPLC) equipped with a spectrophotometric detector (Tosoh ultraviolet-8000, Tosoh, Tokyo, Japan) as described in a previous study [8].

2.7. Assay of IDO activity

IDO activity was assessed using the methylene blue/ascorbate assay, as described previously [15]. Briefly, the liver lysate was centrifuged at 7000 ×*g* at 4 °C for 10 min. The supernatant (50 μL) was then reacted with the substrate solution (50 μL) at 37 °C for 60 min. The substrate solution comprised 100 mM potassium phosphate buffer (pH 6.5), 50 μM methylene blue, 20 μg of catalase, 50 mM ascorbate and 0.4 mM D-tryptophan. After incubation, the samples were acidified with 3% perchloric acid and centrifuged at 7000 ×*g* at 4 °C for 10 min. The concentration of kynurenine in the supernatant of the reaction solution was measured using HPLC, and IDO activity was expressed as the kynurenine content per hour per milligram protein.

2.8. Real-time RT-PCR analysis

Real-time reverse transcription polymerase chain reaction (RT-PCR) was used to quantify the levels of TNF-α, IFN-γ, IL-6, IL-10, MCP-1, and MIP-2 mRNA in the liver. Total RNA in the liver was isolated using Isogen (Nippon Gene, Tokyo, Japan) and reverse-transcribed to cDNA by using a High capacity cDNA transcription kit (Applied Biosystems, Foster City, CA). Purified cDNA was used as the template for real-time RT-PCR conducted with pre-designed primer/probe sets for TNF-α, IFN-γ, IL-6, IL-10, MCP-1, MIP-2 mRNA and 18S rRNA (Applied Biosystems), according to the manufacturer's recommendations. 18S rRNA was used as an internal control. Real-time RT-PCR was carried out using a Light-Cycler 480 system (Roche Diagnostic Systems).

2.9. Western blot analysis

Protein (40 μg) from the liver lysate was subjected to sodium dodecyl sulfate-polyacrylamide gel electrophoresis and then transferred to a nitrocellulose membrane. The membrane was blocked with 5% skim milk and incubated with anti-IDO and anti-β-actin antibodies for 24 h at 4 °C, followed by incubation with peroxidase-labeled anti-rabbit IgG for 60 min at room temperature. Immunoreactive protein bands were visualized using ECL plus (GE Healthcare UK Ltd, England).

2.10. Isolation of liver mononuclear cells and flow cytometry analysis

Hepatic mononuclear cells (MNCs) were isolated as outlined in our previous report [16]. Briefly, the mouse liver tissue was minced using a pair of scissors and the resultant liver homogenate was filtered through a stainless steel mesh. MNCs were obtained by the centrifugation of liver homogenate with Ficoll-Conray (IBL, Gunma, Japan). Flow cytometry was used to evaluate the cell phenotypes in the liver MNCs at 0 h and 24 h after CTL injection. The MNCs were then stained with below-mentioned antibodies: FITC-conjugated hamster anti-mouse CD3ε antibody (clone 145-2C11; BD Biosciences, Franklin Lakes, NJ), FITC-conjugated rat anti-mouse CD4 antibody (clone RM4-5; BD Biosciences), PE-conjugated rat anti-mouse CD8 antibody (clone 53-6.7; BD Biosciences), CD49b PE-conjugated rat anti-mouse CD49b antibody (clone DX5; BD Biosciences) and FITC-conjugated rat anti-mouse F4/80 antibody (clone BM8; eBioscience, San Diego, CA). The phenotypic characterization of the MNCs was carried out using a FACScan flow cytometer (BD Biosciences).

2.11. Measurement of plasma HBsAg level

Plasma HBsAg level was measured using an automated clinical analyzer HISCL 2000i and mouse anti-HBsAg antibody (Sysmex, Kobe, Japan) according to the manufacturer's recommendations.

2.12. Statistical analysis

In each experiment, the results are expressed as mean ± SD. The statistical significance of the difference in mean values was determined using Student's *t* test, and p values less than 0.05 were considered statistically significant.

3. Results

3.1. Up-regulation of IDO expression in the mouse liver following injection of HBV-specific CTL

HBV-specific CTL clones (1×10^6/mouse) were intravenously injected into HBV-Tg/IDO-WT and HBV-Tg/IDO-KO mice. The expression of IDO mRNA in the livers from HBV-Tg/IDO-WT mice was markedly up-regulated mainly at 2 d after CTL injection, whereas that from HBV-Tg/IDO-KO mice was not detected by real-time RT-PCR (Fig. 1A). The IDO protein and activity in the liver tissue from HBV-Tg/IDO-WT mice were also increased 2 d after CTL injection (Fig. 1B, C). Plasma kynurenine concentrations in HBV-Tg/IDO-WT mice were significantly increased relative to those in HBV-Tg/IDO-KO mice at 1 d, 2 d, 4 d, and 7 d after CTL injection (Fig. 1D). These data suggest that IDO expression in the liver was induced after CTL injection, resulting in increased kynurenine production.

3.2. Effects of IDO on liver damage induced by HBV-specific CTL

Plasma ALT levels in HBV-Tg/IDO-KO mice at 1 d and 2 d after CTL injection significantly decreased compared with the levels in HBV-Tg/IDO-WT mice (Fig. 2A). Histological changes were observed in the liver tissues from HBV Tg/IDO-WT and HBV-Tg/IDO-KO mice at 0 d and 2 d after CTL injection. The number of infiltrating cells and necroinflammatory foci in the livers of HBV Tg/IDO-KO mice 2 d after CTL injection was much less than that in the livers of HBV-Tg/IDO-WT mice (Fig. 2B). Moreover, as evaluated by TUNEL staining, a large number of apoptotic hepatocytes were detected in the livers of HBV-Tg/IDO-WT mice at 2 d after CTL injection compared to those found in the livers of HBV-Tg/IDO-KO mice (Fig. 2C).

3.3. Effect of IDO on cytokine and chemokine expression in mouse liver after injection of HBV-specific CTL

Cytokine (TNF-α, IFN-γ, IL-6, IL-10) and chemokine (MCP-1, MIP-2) mRNA expression was determined in the livers of HBV-Tg/IDO-WT and HBV Tg/IDO-KO mice at 0 d, 1 d, 2 d and 7 d following CTL injection. The mRNA expression of TNF-α, IFN-γ, IL-6, MCP-1 and MIP-2 examined in the livers from HBV-Tg/IDO-KO mice was decreased relative to those from the HBV-Tg/IDO-WT mice (Fig. 3A). Additionally, cytokine (TNF-α, IFN-γ) mRNA expression was up-regulated in non-parenchymal cells after CTL injection (Fig. 3B), but there was no significant difference between HBV-Tg/IDO-WT mice and HBV-Tg/IDO-KO mice in cytokine mRNA expression of non-parenchymal cells (Fig. 3B).

3.4. Effect of IDO on the phenotype of MNCs in the liver after injection of HBV-specific CTL

Next, we examined the phenotypes of the MNCs in the livers (CD4+, CD8+, CD3+CD49b−, CD3−CD49b+, CD3+CD49b+ and F4/80+)

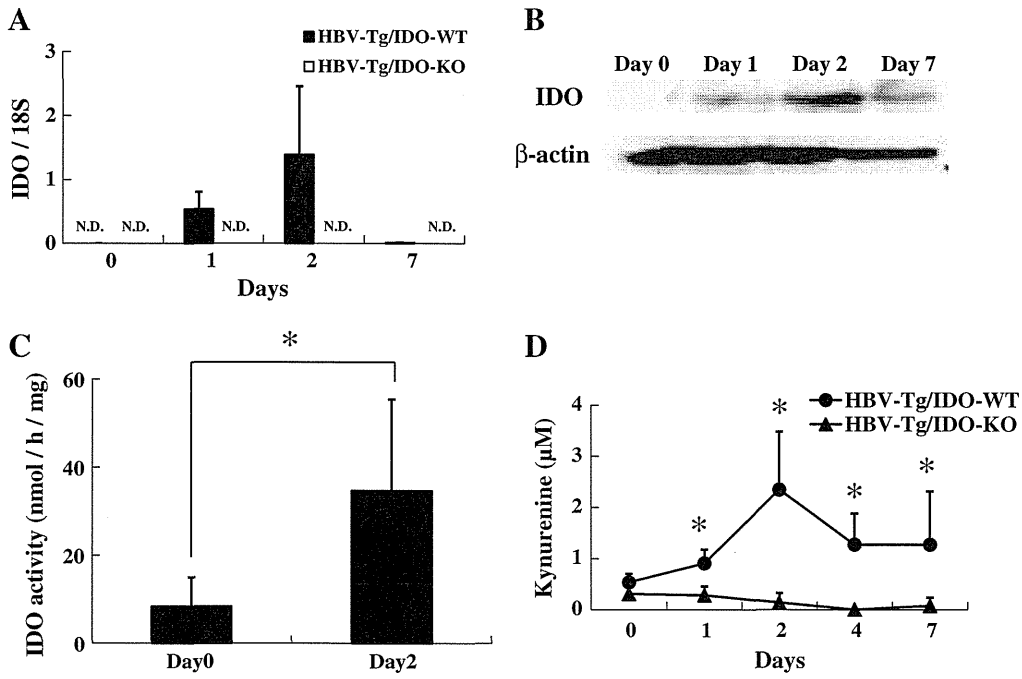

Fig. 1. Increases in IDO expression and activity were observed in HBV-Tg/IDO-WT mice after HBV-specific CTL injection. (A) The relative expression level of IDO mRNA in livers of HBV-Tg/IDO-WT and HBV-Tg/IDO-KO mice administered HBV-specific CTL was measured by quantitative real-time RT-PCR. The resultant data are represented as means ± SD of the results of 4 mice in each group. (B) Expression of IDO protein in the livers of HBV-Tg/IDO-WT mice at 0 d, 1 d, 2 d, and 7 d after HBV-specific CTL injection was examined by western blot analysis and was normalized to β-actin protein. Data are representative of at least 3 independent experiments with similar results. (C) IDO activity in the livers of HBV-Tg/IDO-WT mice at 2 d after receiving HBV-specific CTL injections: Data are represented as mean ± SD of the results from 4 mice in each group. (D) Kynurenine concentrations in plasma were determined using HPLC for HBV-Tg/IDO-WT and HBV-Tg/IDO-KO mice injected with HBV-specific CTL. Data are represented as mean ± SD of the results from 4 mice in each group. *, $p < 0.05$.

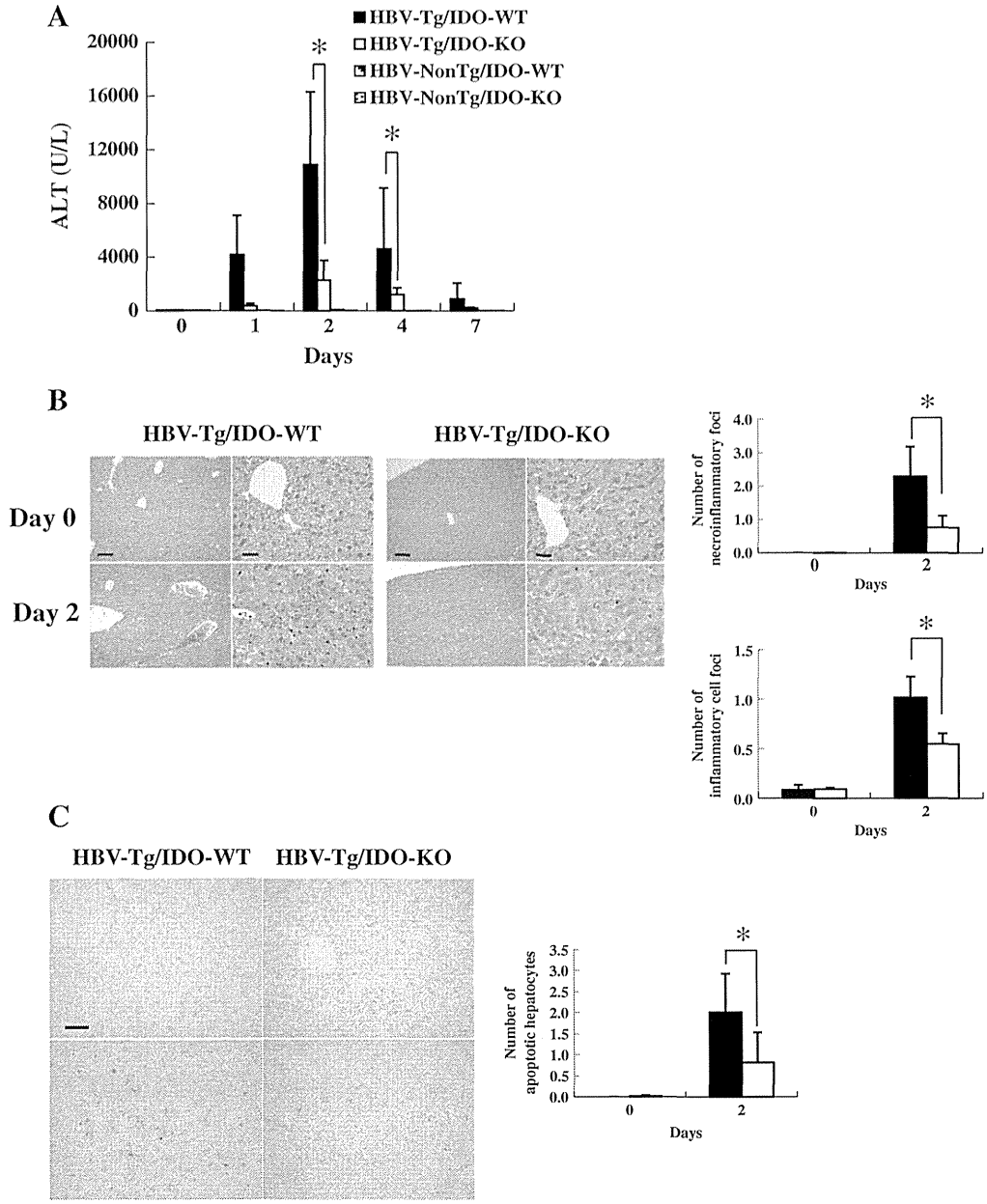

Fig. 2. HBV-specific CTL-induced liver disease in HBV-Tg/IDO-WT mice and HBV-Tg/IDO-KO mice. (A) Plasma ALT levels were analyzed at varying times relative to the injection of 1×10^6 HBV-specific CTL into HBV-Tg/IDO-WT, HBV-Tg/IDO-KO and non-HBV-Tg mice. Data are represented as mean ± SD of the results from 4 mice in each group. (B, C) Histopathological characteristics of HBV-Tg/IDO-WT mice and HBV-Tg/IDO-KO mice. Hematoxylin and eosin staining and TUNEL staining were performed in liver tissues at 2 d after injecting these mice with CTL. Data are represented as mean ± SD of the results from 5 mice in each group. Scale bars, 200 μm (low-power field) and 50 μm (high-power field). *, $p < 0.05$.

of HBV-Tg/IDO-WT mice and HBV Tg/IDO-KO mice at 0 d and 2 d after CTL injection. The total number of MNCs in the livers of HBV-Tg/IDO-WT mice and HBV-Tg/IDO-KO mice was increased at 24 h after CTL injection. The increase in cell number was more reduced in HBV-Tg/IDO-KO mice compared with HBV-Tg/IDO-WT mice. Although there was no significant difference between HBV-Tg/IDO-WT and HBV-Tg/IDO-KO with regard to the number of CD4+, CD8+, CD3+CD49b−, CD3−CD49b+, and CD3+CD49b+ cells at 0 d and 24 h after CTL injection, F4/80+ cells in HBV-Tg/IDO-KO mice significantly decreased compared to those in HBV-Tg/IDO-WT mice at 24 h after the CTL injection (Table 1).

3.5. Effects of 1-MT treatment or kynurenine on liver damage induced by HBV-specific CTL

Because the liver damage in HBV-Tg/IDO-KO mice improved in comparison with that in HBV-Tg/IDO-WT mice, we evaluated the effects of 1-MT, a potent inhibitor of IDO, on liver damage. HBV-Tg/IDO-WT mice were orally administered 1-MT (5 mg/mL) in drinking water for 3 d prior to CTL injection. The plasma ALT levels in HBV-Tg/IDO-WT mice that received 1-MT were significantly decreased compared to HBV-Tg/IDO-WT mice that did not receive 1-MT at 1 d, 2 d and 4 d after CTL injection (Fig. 4A). The number of necroinflammatory foci in the liver of HBV-Tg/IDO-WT mice administered 1-MT at 2 d after CTL injection was lesser than that in the livers of HBV-Tg/IDO-WT mice that were not administered 1-MT, whereas there was no significant difference in inflammatory cell foci with or without the 1-MT administration (Fig. 4B).

HBV-Tg/IDO-KO mice were intraperitoneally administered kynurenine ($50\ mg \cdot kg^{-1} \cdot day^{-1}$) in 0.2 mL of PBS for 7 d after the CTL injection. The plasma ALT level in HBV-Tg/IDO-KO mice that were administered kynurenine was significantly increased compared to that in HBV-Tg/IDO-KO mice that were not administered kynurenine

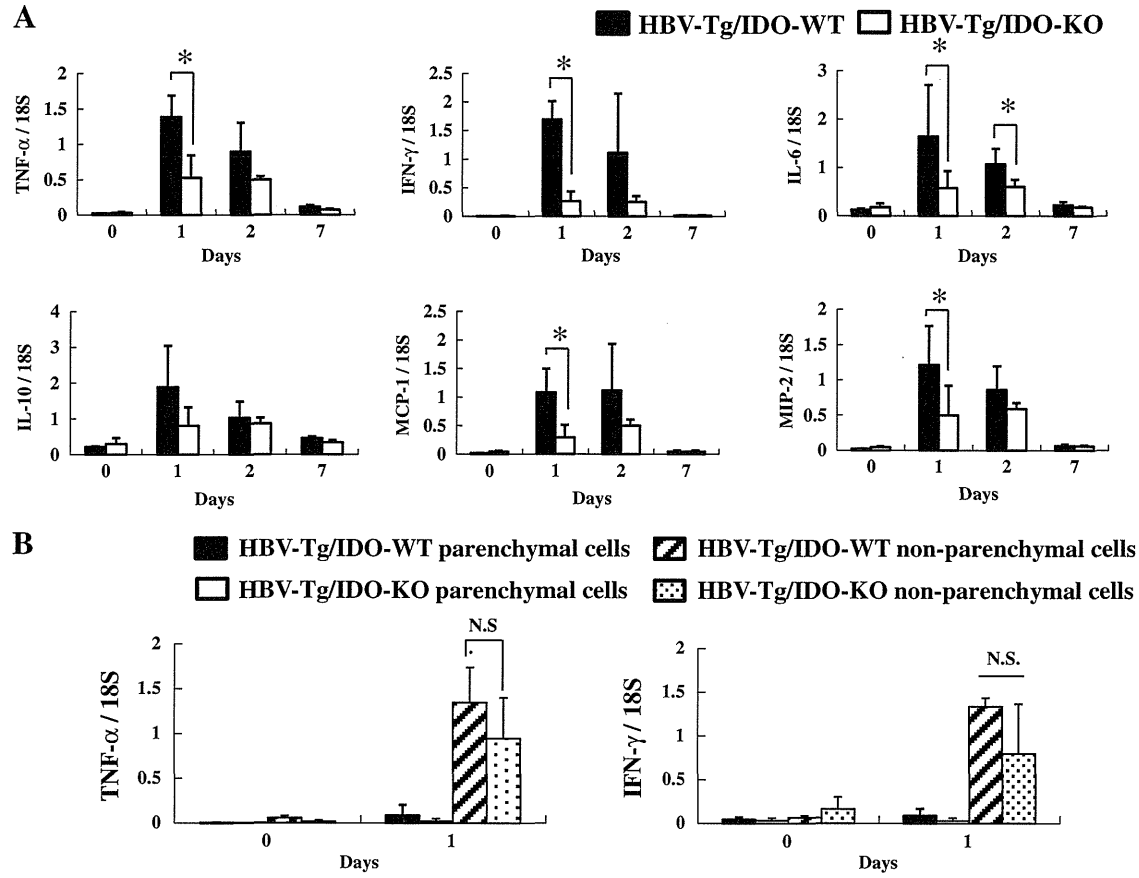

Fig. 3. Cytokine and chemokine expression in the liver tissues of HBV-Tg/IDO-WT and HBV-Tg/IDO-KO mice after HBV-specific CTL injection. (A) TNF-α, IFN-γ, IL-6, IL-10, MCP-1 and MIP-2 mRNA expression was determined in livers from HBV-Tg/IDO-WT and HBV Tg/IDO-KO at 0 d, 1 d, 2 d, and 7 d after CTL injection. Data are represented as mean ± SD of the results from 4 to 6 mice in each group. (B) TNF-α and IFN-γ mRNA expression was determined in parenchymal cells and non-parenchymal cells of livers from HBV-Tg/IDO-WT and HBV Tg/IDO-KO at 0 d and 2 d after CTL injection. Data are represented as mean ± SD of the results from 3 mice in each group. *, $p < 0.05$.

at 2 and 4 d after the CTL injection (Fig. 4C). The number of necroinflammatory foci in the liver of HBV-Tg/IDO-KO mice administered kynurenine at 2 days after the CTL injection was significantly increased compared with those in the liver of HBV-Tg/IDO-KO mice not administered kynurenine, but no significant difference was not confirmed in the inflammatory cell foci with or without the kynurenine administration (Fig. 4D).

3.6. Effect of IDO on circulating HBsAg after injection of HBV-specific CTL

HBsAg expression in HBV-Tg mice may affect the liver damage after CTL injection. Therefore, we next examined plasma HBsAg levels in HBV-Tg/IDO-WT mice and HBV-Tg/IDO-KO mice after CTL injection. There was no difference among HBV-Tg/IDO-WT mice, HBV-Tg/IDO-KO mice and HBV-Tg/IDO-WT mice in plasma HBsAg levels after CTL injection (Fig. 5). It was confirmed that HBsAg was not detected in plasma from non-HBV-Tg mice (data not shown).

3.7. Effect of kynurenine treatment on liver damage and TNF-α mRNA expression induced by recombinant IFN-γ

HBV-Tg/IDO-KO mice were intraperitoneally injected with L-kynurenine (50 $mg \cdot kg^{-1} \cdot day^{-1}$) in 0.2 mL PBS for 2 d after receiving a recombinant IFN-γ injection. Plasma ALT levels in HBV-Tg/IDO-KO mice that were administered L-kynurenine were significantly increased compared to those in HBV-Tg/IDO-KO mice that were not administered kynurenine at 2 d after the recombinant IFN-γ injection (Fig. 6A). Moreover, ALT levels in HBV-Tg/TNF-α-KO mice that were administered L-kynurenine and recombinant IFN-γ were decreased compared to those in HBV-Tg/IDO-KO mice. These data indicated that co-administration of L-kynurenine and recombinant IFN-γ induced

Table 1
The cell number of the MNCs in the livers of HBV-Tg/IDO-WT and HBV-Tg/IDO-KO mice following HBV-specific CTL injection.

	Day 0		Day 1	
	HBV-Tg/IDO-WT	HBV-Tg/IDO-KO	HBV-Tg/IDO-WT	HBV-Tg/IDO-KO
Total cell number ($\times 10^4$)	18.0 ± 2.2	19.3 ± 3.0	33.7 ± 4.7*	27.7 ± 3.6
F4/80+ ($\times 10^4$)	2.6 ± 0.9	2.3 ± 0.5	10.7 ± 1.3*	7.4 ± 1.6
CD4+ ($\times 10^4$)	3.9 ± 1.0	4.5 ± 0.8	4.6 ± 1.3	3.7 ± 0.6
CD8+ ($\times 10^4$)	1.3 ± 0.3	1.7 ± 0.4	2.9 ± 1.2	2.6 ± 0.7
CD3+CD49b− ($\times 10^4$)	3.4 ± 0.6	3.8 ± 0.6	8.0 ± 2.4	6.2 ± 1.3
CD3−CD49b+ ($\times 10^4$)	3.3 ± 0.7	3.0 ± 1.1	8.7 ± 1.5	7.4 ± 1.1
CD3+CD49b+ ($\times 10^4$)	0.8 ± 0.2	0.9 ± 0.4	2.2 ± 0.6	2.1 ± 0.3

Means following the superscript * showed significant differences at $p < 0.05$.

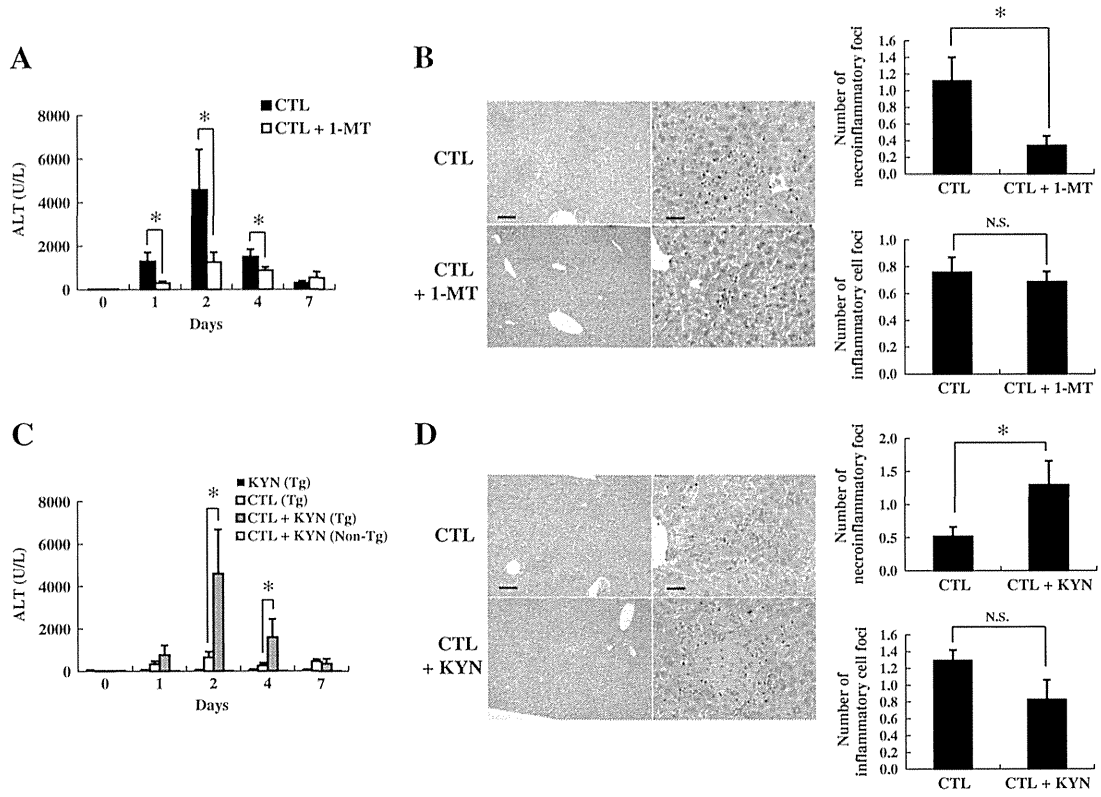

Fig. 4. The effect of 1-MT and kynurenine on liver injury induced by HBV-specific CTL in HBV-Tg mice. (A, B) HBV-Tg/IDO-WT mice were orally administered 1-MT at 0 mg/mL or 5 mg/mL in drinking water for 3 d prior to HBV-specific CTL injection. Plasma ALT levels were analyzed at 0 d, 1 d, 2 d, 4 d, and 7 d after CTL injection. Hematoxylin and eosin staining was performed in mouse liver tissues at 2 d after CTL injection. (C, D) HBV-Tg/IDO-KO mice were injected with HBV-specific CTL followed by intraperitoneal injection with kynurenine (KYN) daily. Plasma ALT levels were analyzed at 0 d, 1 d, 2 d, 4 d, and 7 d after CTL injection (A, C). Hematoxylin and eosin staining was performed in liver tissues at 2 d after CTL injection (B, D). Data are represented as mean ± SD of the results from 4 to 6 mice in each group. *, $p < 0.05$.

liver injury in HBV-Tg and this liver injury depended on TNF-α. TNF-α mRNA expression was significantly up-regulated by recombinant IFN-γ injection in the liver from HBV-Tg/IDO-KO mice, but L-kynurenine administration had no influence on the TNF-α mRNA expression in the liver without IFN-γ injection (Fig. 6B).

4. Discussion

HBV is a DNA virus that is known to infect and cause disease in humans. Infection with HBV is a serious worldwide health problem resulting in fulminant hepatitis, a clinical syndrome consisting of sudden and severe liver injury that leads to hepatic encephalopathy and acute liver failure [1,17,18]. The mortality rate attributed to fulminant hepatitis is approximately 40%. The HBV-Tg mouse model has been useful for defining mechanisms associated with the development of fulminant hepatitis [3–5]. This same mouse model enabled us to

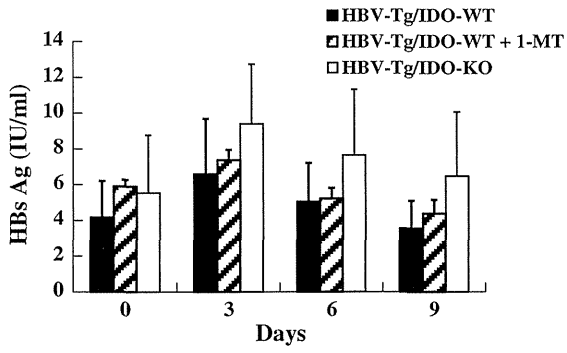

Fig. 5. Effect of IDO on circulating HBsAg after injection with HBV-specific CTL. Plasma HBsAg levels after CTL injection in HBV-Tg/IDO-WT mice with or without 1-MT and HBV-Tg/IDO-KO mice were measured. Data are represented as mean ± SD of the results from 3 to 4 mice in each group.

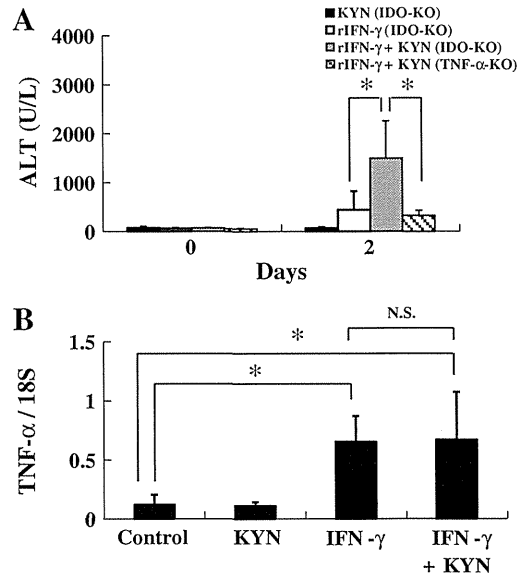

Fig. 6. The effect of recombinant IFN-γ in HBV-Tg mice. (A) HBV-Tg/IDO-KO or HBV-Tg/TNF-α-KO mice were intravenously administered recombinant murine IFN-γ followed by intraperitoneal injections of KYN, and plasma ALT levels in those mice were measured. (B) IFN-γ induced TNF-α mRNA expression in HBV-Tg/IDO-KO with or without KYN treatment was measured. Data are represented as mean ± SD of the results from 3 to 6 mice in each group. *, $p < 0.05$.

investigate the mechanisms underlying the development of fulminant hepatitis as well as to evaluate drug therapies for curing HBV infection. Previously, we had reported that the IDO expression in the hepatocytes was increased in the murine fulminant hepatitis model [7]. IFN-γ induced by HBV-specific CTL enhances the expression of IDO in HBV-Tg mouse hepatocytes. However, the role of enhanced hepatocyte IDO expression following HBV-specific CTL injection is unclear. In this study, we have established an HBV-Tg/IDO-KO mouse strain and evaluated the effects of IDO on liver injury induced by HBV-specific CTL.

IDO is an enzyme that catabolizes tryptophan via the kynurenine pathway to form nicotinic acid, niacin, and nicotinamide adenine dinucleotides. IDO is induced by proinflammatory cytokines, including IFN-γ. Furthermore, IDO is expressed in human and mouse tumor cells, DCs, and macrophages following microbial or viral infections. We recently demonstrated that IDO is induced in the hepatocytes of mice injected with α-galactosylceramide which has an agonistic effect on natural killer T (NKT) cells [19]. Moreover, hepatocyte IDO expression was increased after HBV-specific CTL was administered to the HBV Tg mouse [7]. In the fulminant hepatitis model used in this previous study, IFN-γ directly up-regulated the hepatocyte IDO expression. In our present study, IDO expression was similarly increased in the livers of HBV-Tg/IDO-WT mice following CTL injection, and IDO activity was up-regulated in the liver (Fig. 1). Plasma kynurenine level in HBV-Tg/IDO-WT mice also increased after CTL injection. On the other hand, the expression of IDO mRNA in the liver and plasma kynurenine level were not enhanced by CTL injection in HBV-Tg/IDO-WT mice. Our current data demonstrate that IDO deficiency in the HBV-Tg mice can attenuate liver injury after HBV-specific CTL injection (Fig. 2A and B). Additionally, the number of apoptotic hepatocytes decreased in HBV-Tg/IDO-KO mice compared to HBV-Tg/IDO-WT mice (Fig. 2C). Recent study demonstrated that the enhancement of IDO activity inhibited HBV replication in vitro [20]. HBsAg expression affects liver injury induced by HBV-specific CTL in HBV-Tg mice. In the present model, HBsAg expression was not affected by the suppression of IDO activity in mice after CTL injection (Fig. 5). Therefore, the difference between HBV Tg/WT and HBV Tg/IDO-KO mice in liver injury was not dependent on HBsAg expression in these mice. Real time RT-PCR experiments revealed that the mRNA expression of proinflammatory cytokines and chemokines was decreased in HBV-Tg/IDO-KO mice relative to the HBV-Tg/IDO-WT mice (Fig. 3A). These cytokine expressions were enhanced in non-parenchymal cells but not in hepatocytes. However, there was no significant difference in TNF-α and IFN-γ mRNA expression after CTL injection between HBV-Tg/IDO-WT and HBV-Tg/IDO-KO mice (Fig. 3B). The difference in infiltrating cell number between HBV-Tg/IDO-WT and HBV-Tg/IDO-KO mice contributes to the difference in inflammatory cytokine expression in the whole liver (Table 1). The reduction on the expression of these cytokines and chemokines in the liver indicated that the inflammation in the liver of HBV-Tg/IDO-KO mice administered CTL was decreased. In general, increased hepatic IDO expression induces apoptosis in activated T cells and NK cells [21]. Our previous report has also shown that the number of activated lymphocytes in WT mice is obviously decreased compared to those in IDO-KO mice in α-galactosylceramide-induced hepatitis model [19]. Several studies have shown that tryptophan metabolites can induce apoptosis in some kinds of cells in vitro and in vivo [21–23]. IDO exerts an immunosuppressive effect via the induction of apoptosis in T cells and NK cells. Moreover, tryptophan metabolites (including kynurenine, 3-hydroxy-kynurenine, 3-hydroxyanthranilic acid, and quinolinic acid) produced by IDO catalysis have neurotoxic effects [24,25]. Our current data also indicate that tryptophan metabolites, in particular kynurenine, can aggravate liver injury in HBV-Tg mice following HBV-specific CTL injection (Fig. 4C, D). However, administering kynurenine alone did not promote liver injury in the HBV-Tg mice (Fig. 4C and D). HBV-specific CTL injection was also required to induce the observed hepatotoxicity caused by kynurenine in HBV-Tg mice. In this hepatitis model, the increase of IFN-γ production after HBV-specific CTL injection is required for the progression of liver injury. Our results strongly suggested that IFN-γ in cooperation with kynurenine is involved in liver injury induced by HBV-specific CTL. Previously our study demonstrated that TNF-α also deeply contributes to liver injury promoted by HBV-specific CTL [7]. The progression of liver injury depended on the TNF-α produced by non-HBsAg-specific inflammatory cells stimulated with IFN-γ. TNFR1 expression in hepatocytes was up-regulated after HBV-specific CTL injection, and it was considered that hepatocytes became more susceptible to TNF-α after CTL injection [4]. Therefore, the effect of the administration with IFN-γ and kynurenine was examined in HBV-Tg/TNF-α-KO mice. The liver injury induced by HBV-specific CTL in HBV-Tg/TNF-α-KO mice significantly improved compared to that in HBV-Tg/IDO-KO mice (Fig. 6A). These data suggested that TNF-α is also involved in IFN-γ and kynurenine induced liver injury in HBV-Tg mice. Moreover, IFN-γ increased the expression of TNF-α with or without kynurenine in HBV-Tg/IDO-KO mice (Fig. 6B). We suspected that the cooperative effect of TNF-α from non-HBsAg-specific inflammatory cells stimulated with IFN-γ and the increase of kynurenine in the liver are critical on the accomplishment of acute liver injury. Recent report demonstrated that the livers of HBV-Tg mice are susceptible to liver injury by some cytokines (IFN-γ and TNF-α) because of the accumulation of HBV antigens [26]. Therefore, IDO activity and expression should be suppressed in viral hepatitis to reduce liver injury. Our present results suggest that 1-MT can reduce liver injury in HBV-Tg mice administered HBV-specific CTL (Fig. 4A and B). 1-MT may be available in clinical therapy for severe acute hepatitis caused by HBV infection.

5. Conclusion

In conclusion, we have found that IDO deficiency attenuated liver injury in HBV-Tg mice injected with HBV-specific CTL, which caused HBV-specific CTL and other immune cells in the liver to secrete a large amount of IFN-γ. Hepatocytes with accumulated HBV antigen are susceptible to apoptosis in the simultaneous presence of both IFN-γ and kynurenine. The observed reduction in IDO activity following 1-MT treatment could facilitate the development of effective therapies for patients with fulminant hepatitis caused by HBV infection.

Conflict of interest

None declared.

Acknowledgements

We thank Francis V. Chisari (of The Scripps Research Institute) for providing the HBV-Tg mice. This work was supported by Grants-in-Aid for JSPS Fellows (10 J06850) from the Ministry for Education, Culture, Sports, Science, and Technology of Japan.

References

[1] T.L. Wright, J.Y. Lau, Clinical aspects of hepatitis B virus infection, Lancet 342 (1993) 1340–1344.
[2] L.G. Guidotti, F.V. Chisari, Immunobiology and pathogenesis of viral hepatitis, Annu. Rev. Pathol. 1 (2006) 23–61.
[3] K. Ando, T. Moriyama, L.G. Guidotti, S. Wirth, R.D. Schreiber, H.J. Schlicht, S.N. Huang, F.V. Chisari, Mechanisms of class I restricted immunopathology. A transgenic mouse model of fulminant hepatitis, J. Exp. Med. 178 (1993) 1541–1554.
[4] H. Ito, K. Ando, T. Ishikawa, K. Saito, M. Takemura, M. Imawari, H. Moriwaki, M. Seishima, Role of TNF-alpha produced by nonantigen-specific cells in a fulminant hepatitis mouse model, J. Immunol. 182 (2009) 391–397.
[5] K. Ando, L.G. Guidotti, S. Wirth, T. Ishikawa, G. Missale, T. Moriyama, R.D. Schreiber, H.J. Schlicht, S.N. Huang, F.V. Chisari, Class I-restricted cytotoxic T lymphocytes are directly cytopathic for their target cells in vivo, J. Immunol. 152 (1994) 3245–3253.
[6] L.G. Guidotti, T. Ishikawa, M.V. Hobbs, B. Matzke, R. Schreiber, F.V. Chisari, Intracellular inactivation of the hepatitis B virus by cytotoxic T lymphocytes, Immunity 4 (1996) 25–36.

[7] N. Iwamoto, H. Ito, K. Ando, T. Ishikawa, A. Hara, A. Taguchi, K. Saito, M. Takemura, M. Imawari, H. Moriwaki, M. Seishima, Upregulation of indoleamine 2,3-dioxygenase in hepatocyte during acute hepatitis caused by hepatitis B virus-specific cytotoxic T lymphocytes in vivo, Liver Int. 29 (2009) 277–283.
[8] S. Fujigaki, K. Saito, K. Sekikawa, S. Tone, O. Takikawa, H. Fujii, H. Wada, A. Noma, M. Seishima, Lipopolysaccharide induction of indoleamine 2,3-dioxygenase is mediated dominantly by an IFN-gamma-independent mechanism, Eur. J. Immunol. 31 (2001) 2313–2318.
[9] H.W. Murray, A. Szuro-Sudol, D. Wellner, M.J. Oca, A.M. Granger, D.M. Libby, C.D. Rothermel, B.Y. Rubin, Role of tryptophan degradation in respiratory burst-independent antimicrobial activity of gamma interferon-stimulated human macrophages, Infect. Immun. 57 (1989) 845–849.
[10] Y. Wang, J.R. Jacob, S. Menne, C.A. Bellezza, B.C. Tennant, J.L. Gerin, P.J. Cote, Interferon-gamma-associated responses to woodchuck hepatitis virus infection in neonatal woodchucks and virus-infected hepatocytes, J. Viral Hepat. 11 (2004) 404–417.
[11] K. Mohib, Q. Guan, H. Diao, C. Du, A.M. Jevnikar, Proapoptotic activity of indoleamine 2,3-dioxygenase expressed in renal tubular epithelial cells, Am. J. Physiol. Renal. Physiol. 293 (2007) F801–F812.
[12] L.K. Jasperson, C. Bucher, A. Panoskaltsis-Mortari, P.A. Taylor, A.L. Mellor, D.H. Munn, B.R. Blazar, Indoleamine 2,3-dioxygenase is a critical regulator of acute graft-versus-host disease lethality, Blood 111 (2008) 3257–3265.
[13] T. Taniguchi, M. Takata, A. Ikeda, E. Momotani, K. Sekikawa, Failure of germinal center formation and impairment of response to endotoxin in tumor necrosis factor alpha-deficient mice, Lab. Invest. 77 (1997) 647–658.
[14] H. Ito, K. Ando, T. Ishikawa, T. Nakayama, M. Taniguchi, K. Saito, M. Imawari, H. Moriwaki, T. Yokochi, S. Kakumu, M. Seishima, Role of Valpha14+ NKT cells in the development of Hepatitis B virus-specific CTL: activation of Valpha14+ NKT cells promotes the breakage of CTL tolerance, Int. Immunol. 20 (2008) 869–879.
[15] H. Ohtaki, H. Ito, K. Ando, T. Ishikawa, M. Hoshi, R. Tanaka, Y. Osawa, T. Yokochi, H. Moriwaki, K. Saito, M. Seishima, Interaction between LPS-induced NO production and IDO activity in mouse peritoneal cells in the presence of activated Valpha14 NKT cells, Biochem. Biophys. Res. Commun. 389 (2009) 229–234.
[16] H. Ohtaki, H. Ito, K. Ando, T. Ishikawa, K. Saito, M. Imawari, T. Yokochi, H. Moriwaki, M. Seishima, Valpha14 NKT cells activated by alpha-galactosylceramide augment lipopolysaccharide-induced nitric oxide production in mouse intra-hepatic lymphocytes, Biochem. Biophys. Res. Commun. 378 (2009) 579–583.
[17] T.J. Liang, Hepatitis B: the virus and disease, Hepatology 49 (2009) S13–S21.
[18] R.A. Meyer, M.C. Duffy, Spontaneous reactivation of chronic hepatitis B infection leading to fulminant hepatic failure. Report of two cases and review of the literature, J. Clin. Gastroenterol. 17 (1993) 231–234.
[19] H. Ito, M. Hoshi, H. Ohtaki, A. Taguchi, K. Ando, T. Ishikawa, Y. Osawa, A. Hara, H. Moriwaki, K. Saito, M. Seishima, Ability of IDO to attenuate liver injury in alpha-galactosylceramide-induced hepatitis model, J. Immunol. 185 (2010) 4554–4560.
[20] R. Mao, J. Zhang, D. Jiang, D. Cai, J.M. Levy, A. Cuconati, T.M. Block, J.T. Guo, H. Guo, Indoleamine 2,3-dioxygenase mediates the antiviral effect of gamma interferon against hepatitis B virus in human hepatocyte-derived cells, J. Virol. 85 (2011) 1048–1057.
[21] G. Frumento, R. Rotondo, M. Tonetti, G. Damonte, U. Benatti, G.B. Ferrara, Tryptophan-derived catabolites are responsible for inhibition of T and natural killer cell proliferation induced by indoleamine 2,3-dioxygenase, J. Exp. Med. 196 (2002) 459–468.
[22] T. Morita, K. Saito, M. Takemura, N. Maekawa, S. Fujigaki, H. Fujii, H. Wada, S. Takeuchi, A. Noma, M. Seishima, 3-Hydroxyanthranilic acid, an L-tryptophan metabolite, induces apoptosis in monocyte-derived cells stimulated by interferon-gamma, Ann. Clin. Biochem. 38 (2001) 242–251.
[23] P. Terness, T.M. Bauer, L. Rose, C. Dufter, A. Watzlik, H. Simon, G. Opelz, Inhibition of allogeneic T cell proliferation by indoleamine 2,3-dioxygenase-expressing dendritic cells: mediation of suppression by tryptophan metabolites, J. Exp. Med. 196 (2002) 447–457.
[24] T.J. Connor, N. Starr, J.B. O'Sullivan, A. Harkin, Induction of indolamine 2,3-dioxygenase and kynurenine 3-monooxygenase in rat brain following a systemic inflammatory challenge: a role for IFN-gamma? Neurosci. Lett. 441 (2008) 29–34.
[25] D.J. Bonda, M. Mailankot, J.G. Stone, M.R. Garrett, M. Staniszewska, R.J. Castellani, S.L. Siedlak, X. Zhu, H.G. Lee, G. Perry, R.H. Nagaraj, M.A. Smith, Indoleamine 2,3-dioxygenase and 3-hydroxykynurenine modifications are found in the neuropathology of Alzheimer's disease, Redox Rep. 15 (2010) 161–168.
[26] P.N. Gilles, D.L. Guerrette, R.J. Ulevitch, R.D. Schreiber, F.V. Chisari, HBsAg retention sensitizes the hepatocyte to injury by physiological concentrations of interferon-gamma, Hepatology 16 (1992) 655–663.

Journal of Virological Methods 207 (2014) 169–177

Contents lists available at ScienceDirect

Journal of Virological Methods

journal homepage: www.elsevier.com/locate/jviromet

High-throughput and sensitive next-generation droplet digital PCR assay for the quantitation of the hepatitis C virus mutation at core amino acid 70

Motokazu Mukaide[a,b], Masaya Sugiyama[a], Masaaki Korenaga[a,*], Kazumoto Murata[a], Tatsuya Kanto[a], Naohiko Masaki[a], Masashi Mizokami[a]

[a] Research Center for Hepatitis and Immunology, National Center for Global Health and Medicine, 1-7-1 Kohonodi, Ichikawa, Chiba 272-8516 Japan
[b] Research and development department, SRL, Inc., 5-6-50 Shin, Hino, Tokyo 191-0002, Japan

Article history:
Received 12 November 2013
Received in revised form 2 July 2014
Accepted 4 July 2014
Available online 11 July 2014

Keywords:
HCV
Core a.a.70
Ultra-deep pyrosequencing
ddPCR

ABSTRACT

The next-generation droplet digital polymerase chain reaction (ddPCR) assay employs an emulsion-based endpoint to quantitate the amount of target DNA and is more robust than real-time PCR when analyzing sequence variations. However, no studies have applied this technique to quantitate mutations in polymorphic viral genomes. To develop this approach, a ddPCR-based assay was designed to quantitate with high-throughput and sensitivity mutations and their frequencies in codon 70 of the hepatitis C virus (HCV) gene that encodes the Core protein. The assay was linear from 2.5 to 10^5 copies per assay, and the limit of detection of mutants in the presence of a 20,000-fold excess of wild type was 0.005%. The results correlated well with those obtained using the COBAS® TaqMan® HCV Test, which is a real-time PCR assay for the quantitative detection of HCV RNA in human serum ($n = 87$; range, 2.3–7.7 $\log_{10}$ IU/mL; Pearson's $R^2 = 0.9120$; $p < 0.0001$). The median frequencies of mutations by ddPCR were 0.262% ($n = 55$; range, 0–37.951%) and 99.687% ($n = 32$; range, 52.191–100%) for the wild-type and mutant sequences, respectively, by direct sequencing. The ddPCR assay should be useful for quantitating mutations in other polymorphic viral genomes.

1. Introduction

The development of quantitative polymerase chain reaction (qPCR) technology has a rich and diverse history (Syvänen et al., 1988; Becker-andr and Hahlbrock, 1989; Gilliland et al., 1990; Porcher et al., 1992). Over the past few decades, the overwhelming majority of qPCR technology has relied on some version of real-time PCR using TaqMan® probe (Higuchi et al., 1993). However, the accuracy of real-time PCR is limited by relative quantitation using a standard curve, and this technique cannot detect less than 1% mutant DNA in a wild-type DNA background (Hindson et al., 2011). In 1999, digital PCR (dPCR) (Vogelstein and Kinzler, 1999) was developed for the absolute quantitation of target DNA. This technique does not require generation of a standard curve by the real-time PCR. Recently, new next-generation digital PCR-droplet PCR (ddPCR) has been developed, which is more precise than the real-time PCR (Morisset et al., 2013; Strain et al., 2013) as a high-throughput assay using conventional TaqMan assays with a 96-well plate format (Hindson et al., 2011).

On the other hand, the mutation rate of RNA viruses is high, ranging from 10^{-1} to 10^{-4} base substitutions per genome per year (Holland et al., 1982), because of the absence of proofreading enzymes that assure the fidelity of DNA replication. This high mutation frequency is coupled with high replication rates. The rates of viral genomic RNA mutation exceed those of chromosomal mutations of the host by a factor of one million. The ddPCR proved useful for the quantitative detection of single nucleotide polymorphisms in the human genome (BRAF-V600E, EGFR, and KRAS) (Hindson et al., 2011; Pekin et al., 2011; Hubers et al., 2013), but its application to quantification of highly polymorphic viral genome mutations has not been reported.

The hepatitis C virus (HCV) is an RNA virus of the family Flaviviridae, genus *Hepacivirus*, and it infects approximately 185 million people worldwide, with 3–4 million new infections annually (Thomas, 2013). Persistent HCV infection is usually clinically mild, but 20% of infections progress to severe chronic hepatitis and cirrhosis that occasionally culminate in hepatocellular carcinoma (HCC) (Niederau et al., 1998; Liang et al., 2000). More than

* Corresponding author. Tel.: +81 47 372 3501; fax: +81 47 375 4746.
E-mail address: dmkorenaga@hospk.ncgm.go.jp (M. Korenaga).

http://dx.doi.org/10.1016/j.jviromet.2014.07.006
0166-0934/

350,000 people die each year from HCV-related liver failure and HCC (Kiyosawa et al., 1990; Yang and Roberts, 2010). The HCV genome consists of a 9.6-kb RNA with a large open reading frame that encodes a polyprotein of 3010 amino acids (Grakoui et al., 1993). Putative structural proteins, located in the N-terminal one-fourth of the polyprotein, include the capsid protein (Core protein), followed by two possible virion envelope proteins (E1 and E2) and nonstructural proteins (NS), including NS2, NS3, NS4A, NS4B, NS5A, and NS5B, which are required for RNA replication. A mutation in the sequence of amino acid 70, encoding the Core protein (Core a.a.70), is associated with the progression of liver disease and is an independent risk factor for the development of HCC (Miura et al., 2011, 2013; Akuta et al., 2012). Although the mutation can generally be detected by direct sequencing (Akuta et al., 2005), it is difficult to determine the presence of substitutions when the sequencing data are superimposed. This has hindered attempts to elucidate the relationship between the progression of liver disease and mutations in the HCV genome. Ultra-deep pyrosequencing (UDPS) results show that 89.9% hepatitis C viruses harbor mutations in the genomes (Miura et al., 2013). However, performing UDPS analysis requires skill, considerable effort, and does not generate sufficiently reproducible and accurate data (Noguchi et al., 2006; Hoff, 2009; Glenn, 2011).

As mentioned earlier, ddPCR can be used for the quantitative detection of single nucleotide polymorphisms in the human genome (Hindson et al., 2011; Pekin et al., 2011; Hubers et al., 2013). However, its application for the quantitation of mutations in highly polymorphic viral genomes (such as those of HIV and HCV) has not been reported. Therefore, the goal of the present study was to design a novel ddPCR assay to quantitate mutations in HCV Core a.a.70.

2. Materials and methods

2.1. Sample collection

From May 2011 through May 2013, serum samples were obtained from 87 to 69 patients infected with HCV-1b. The patients were from a hospital in Japan, which was located within the same premises as our participating institutions. The serum samples were stored at −80 °C for further use. All patients were positive for antibodies against HCV antigen (anti-HCV) and for HCV RNA. To confirm false positives in the ddPCR assay, twenty clones in 32 clinical samples were picked up and analyzed the frequency of aa70 mutations by direct sequencing (Supplementary data 1), and seven samples, which were HCV RNA negative using the COBAS TaqMan® HCV Test, were used (Supplementary data 2). Two different sample groups were used in the assay to alleviate bias. The first group of 87 samples (38% were obtained from men; mean age, 67.0 ± 12.28 years) was used for design purposes, and the other group of 69 samples (Supplementary data 3; 34% were obtained from men; mean age, 54.5 ± 10.13 years) was used for validation purposes. The ethics committees of the participating institutions approved the study protocol, which conforms to the 2008 Declaration of Helsinki. Written informed consent was obtained from each patient.

2.2. RNA extraction and cDNA synthesis

Total nucleic acids from clinical samples were isolated using the MagNA Pure LC Total Nucleic Acid Isolation Kit-High Performance (Roche Diagnostics, Tokyo, Japan) on a MagNA Pure LC 2.0 instrument (Roche Diagnostics), according to the external lysis protocol provided by the manufacturer (Edelmann et al., 2013). HCV RNA was extracted from 0.5 mL of serum and eluted in 0.05 mL of elution buffer included in the kit. cDNA synthesis was performed using SuperScript III reverse transcriptase (Invitrogen, Carlsbad, CA, USA) with random primers, following the manufacturer's protocol.

2.3. Detection of mutations in Core a.a.70 using direct nucleotide sequence analysis

The Core gene was amplified using nested PCR and sequenced using the BigDye Terminator V3.1 Cycle Sequencing Kit and Genetic Analyzer 3130xl (Life Technologies, Tokyo, Japan). The Core a.a.70 substitutions were identified as described by Akuta et al. (2005).

2.4. Production of a plasmid standard

The amplicons containing the region encompassing wild-type and mutant Core a.a.70 sequences (nucleotide position: 330–684 bp) were cloned into the pCR4-TOPO vector (Life Technologies, Japan), and the identities of eight clones were verified by nucleotide sequencing. The concentration of plasmid DNA was measured using a Nanoview Spectrophotometer (GE Healthcare, Baie d'Urfe, Quebec, Canada), and optical density (OD) at 260 nm and the ratio of ODs at 260/280 nm, respectively, were used to determine the quantity and purity of plasmid DNA. The initial copy number of standard plasmids per microliter was calculated using a DNA copy number calculator (Thermo Scientific, 2013). Serial dilutions of plasmid DNA were prepared in Easy Dilution Solution (Takara Bio, Otsu, Japan).

2.5. Analysis of Core a.a.70 and assay design

Direct nucleotide sequence analysis of the 87 patients with HCV infection was performed to determine mutation patterns in and around the target Core a.a.70 site. Throughout this article, the nucleotide positions of the amino acids were numbered according to the full-length genome sequence of HCV genotype 1b strain NC1 (GenBank accession number AB691953.1). Different complex patterns of mutations were revealed; however, polymorphisms within 13 nucleotides (544–556 bp) up- or downstream of the target codon were limited to seven patterns. Bases presented in italics indicate mutations and those underlined indicate the codon of Core a.a.70 (Table 1). The Mutant type changed from arginine to glutamine (pattern 3 and 4) or histidine (pattern 7) at position 70 of amino acids encoding the HCV Core protein. The sequence of Core a.a.70 obtained from 84 of the 87 patients (96.55%) included the top 1–4 nucleic acid sequence patterns. These common sequences were confirmed in 69 patients with HCV infection (Supplementary data 3). Real-time PCR primers were designed according to the conserved sequences using DNA database (Hepatitis Virus DataBase Server, http://s2as02.genes.nig.ac.jp/) and PrimerExpress 3.0 software (Applied Biosystems, Foster City, CA, USA) as follows: sense, 5′-CGT GGA AGG CGR CAA CCT AT-3′ (516–535 bp); antisense, 5′-CRC GGG GKG ACA GGA GCC A-3′ (645–627 bp). Fluorescence resonance energy transfer probe sequences were designed according to the sequence patterns (Table 1 and Supplemental data 3) as follows: 5′-VIC-CTCGCCGRCCCGA-MGB-3′ (wild-type probe: 544–556 bp) for detecting the wild-type sequences and 5′-FAM-CTCGCCARCCCGA-MGB-3′ (mutant probe: 544–556 bp) for detecting the mutant sequences.

2.6. ddPCR

The QX100™ Droplet Digital™ PCR System (BioRad, Hercules, CA, USA) was used according to the manufacturer's instructions. The reaction mixtures for ddPCR contained the following components: 10 μL of ddPCR Master Mix (Bio-Rad, Pleasanton, CA, USA), 3 μL of primers (final concentration, 900 nM each), 2 μL of probes